Biophysical Chemistry 175–176 (2013) 1–16

Contents lists available at SciVerse ScienceDirect

Biophysical Chemistry

journal homepage: http://www.elsevier.com/locate/biophyschem

Appraisal of sildenafil binding on the structure and promiscuous esterase activity of native and histidine-modified forms of carbonic anhydrase II

Hamid Mahdiuni [a,1], Nooshin Bijari [b,1], Masoud Varzandian [a], Seyyed Abolghasem Ghadami [a,b], Mozafar Khazaei [c], Mohammad Reza Nikbakht [d,*], Reza Khodarahmi [b,d,*]

[a] Department of Biology, Faculty of Science, Razi University, Kermanshah, Iran
[b] Medical Biology Research Center, Kermanshah University of Medical Sciences, Kermanshah, Iran
[c] Fertility and Infertility Research Center, Kermanshah University of Medical Sciences, Kermanshah, Iran
[d] Faculty of Pharmacy, Kermanshah University of Medical Sciences, Kermanshah, Iran

HIGHLIGHTS

- Modification of exposed histidines decreased esterase activity of the enzyme.
- Sildenafil–CA interaction induces protein conformational changes.
- Sildenafil binding induced reorganization of hydrogen bonds within CA active site.
- Sildenafil binding may change hydration positions on the CA surface.

GRAPHICAL ABSTRACT

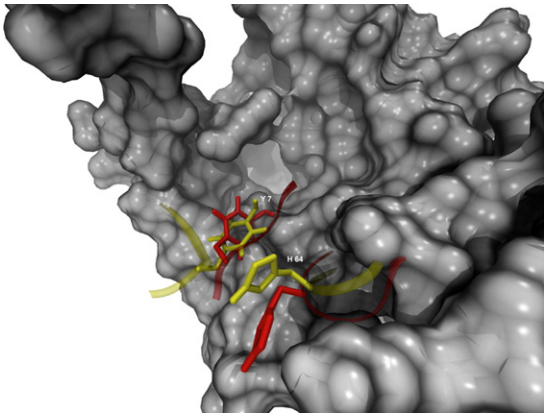

ARTICLE INFO

Article history:
Received 24 December 2012
Received in revised form 8 February 2013
Accepted 12 February 2013
Available online 19 February 2013

Keywords:
Carbonic anhydrase
Sildenafil
Enzyme activator
Diethyl pyrocarbonate
Chemical modification

ABSTRACT

Sildenafil was investigated for its interaction with the native and modified human carbonic anhydrase II (hCA II). Modification of exposed histidine side chains with diethyl pyrocarbonate decreased esterase activity of the enzyme. The treatment of both native and modified CA with sildenafil revealed slight and moderate enzyme activation profiles, respectively. In addition, in the present study the effects of sildenafil on the structural properties of native and modified hCA II were investigated employing different computer simulation and spectroscopic techniques such as UV–vis, circular dichroism (CD), fluorescence spectroscopy and molecular dynamics. Fluorescence measurements showed that the sildenafil acts as a quencher of the native and modified enzyme fluorescence. Stern–Volmer analyses revealed the existence of one binding site on the native/modified enzyme for sildenafil. The thermodynamic parameters, enthalpy change (ΔH) and entropy change (ΔS) of drug binding were not also similar, which indicate that different interactions are responsible in CA–drug interaction. Calculation of the protein surface hydrophobicity (PSH), using 1,8-Anilinonaphtalene Sulfonate (ANS), indicated the increment of PSH of native and modified hCA II in the presence of sildenafil. Overall, sildenafil–CA interaction probably induces protein conformational changes and completes reorganization of both hydrogen bond networks within the active site cavity and hydration positions on the protein surface.

Abbreviations: hCA, human carbonic anhydrase; PDE5, phosphodiesterase-5; CD, circular dichroism; PSH, protein surface hydrophobicity; ANS, 1,8-anilinonaphtalene sulfonate; PDB, protein data bank; ED, erectile dysfunction; CAIs, CA inhibitors; DEPC, diethyl pyrocarbonate; *p*-NPA, *p*-nitrophenyl acetate; DLS, dynamic light scattering; SAS, solvent accessible surface; SES, solvent excluded surface; CEt, carbethoxy; FCEt, formyl-biscarbethoxy; UCEt, urethane-carbethoxy.

* Corresponding authors at: Faculty of Pharmacy, Kermanshah University of Medical Sciences, Kermanshah, Iran. Tel.: +98 831 4276473; fax: +98 831 4276471.
E-mail addresses: rkhodarahmi@mbrc.ac.ir, rkhodarahmi@kums.ac.ir (R. Khodarahmi), drnikbakht@kaums.ac.ir, mnikbakht2001@yahoo.com (M.R. Nikbakht).

[1] These two authors contributed equally to this work.

0301-4622/$ – see front matter © 2013 Elsevier B.V. All rights reserved.
http://dx.doi.org/10.1016/j.bpc.2013.02.003

1. Introduction

Carbonic anhydrase (CA, EC 4.2.1.1) enzymes are diffusion-controlled metalloenzymes that catalyze the reversible hydration of carbon dioxide to bicarbonate and hydrogen ions [1]. At least 16 different carbonic anhydrase isoforms were isolated in higher vertebrates. These isozymes have diversified tissue distribution and subcellular positions and they exist in archaea, eubacteria, animals and plants [2]. Some of these are involved in crucial physiological processes such as respiration, acid–base balance, calcification, electrolytes secretion, biosynthetic reactions (including gluconeogenesis, lipogenesis and ureagenesis) [3]. The CAII isozyme, a functional 29-kD (and monomer) polypeptide is the fastest and most widespread isoform. Key features of the enzyme active site which is located at the bottom of a 15-Å cone shaped cavity, (Fig. 1A) include a zinc ion coordinated tetrahedrally by 3 histidine residues (His_{94}, His_{96} and His_{119}) and a water molecule/hydroxide ion as a fourth ligand (water 263). The generally accepted catalytic mechanism of carbonic anhydrase is described by a 3-step kinetic scheme (I): the substrate is subjected to a nucleophilic attack by a Zn-coordinated OH^- moiety which catalyzes the interconversion of CO_2 to HCO_3^-, leaving a water molecule as the fourth zinc-bound water; (II) an intramolecular proton transfer takes place from the zinc-bound catalytic water (Water 263, see Fig. 1A) to the imidazole ring of His_{64}; and (III) an intermolecular proton transfer from His-64 to the surrounding solvent (Eqs. (a)–(c), see below) [4,5].

$$His_{64}-E-Zn-OH^- + CO_2 + H_2O \leftrightarrows His_{64}-E-Zn-HCO_3^- + H_2O \rightleftarrows His_{64}-E-Zn-H_2O + HCO_3^- \quad (a)$$

$$His_{64}-E-Zn-H_2O \leftrightarrows H_3O^+ - His_{64}-E-Zn-OH^- \quad (b)$$

$$H_3O^+ - His_{64}-E-Zn-OH^- + H_2O \leftrightarrows His_{64}-E-Zn-OH^- + H_3O^+ \quad (c)$$

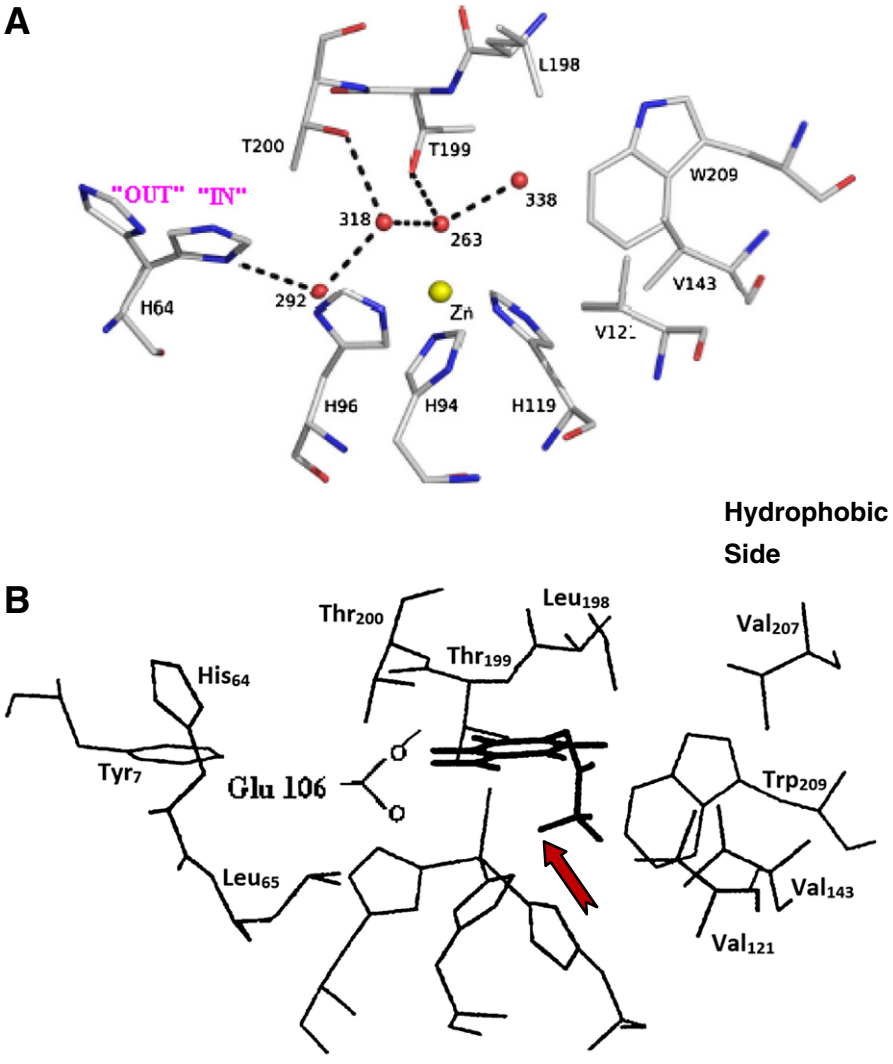

Fig. 1. (A) Diagrammatic representation of the active site and proton transfer paths identified in wild-type CA II. The zinc ion is tetrahedrally coordinated by 3 histidines (His_{94}, His_{96}, and His_{119}) and catalytic water (Water 263). The deep water (Water 338) sits in a hydrophobic pocket lined by Leu_{198}, Trp_{209}, Val_{143}, and Val_{121} at the bottom of the active site. Water 318 is in a hydrophilic environment toward the mouth of the active site cone. The proton shuttle His_{64}, shown in both "in/inward" and "out/outward" positions, is linked via Water 292 and Water 318 to the catalytic water. The side chain of His_{64} residue points towards the active site in the "inward" conformer, while it is orientated away from the active site towards the surface of the protein in the "outward" conformation. Hydrogen bonds are depicted as dotted lines, and waters are labeled with numbers only. Numbering is according to PDB code 2CBA (adapted from [17]). (B) Hypothetical model of the position of ester substrates (red arrow) in the active site of human CA II. See the Glu_{106} position.
(Adopted from [11,12], also see Fig. 10).

As indicated in Eqs. (a)–(c), in the reverse path, the mechanism of CA action requires an excess proton to be delivered to the active site of the enzyme from its surface. The rate limiting step in CA-mediated reaction is the shuttling of protons between the catalytic center of the enzyme and the bulk solution as it determines how quickly the enzyme will once again be ready to catalyze the conversion of CO_2. Different kinetic studies indicate that in a well-buffered solution, the intramolecular proton transfer is rate determining [4,6]. It has also been shown that, in CA II, this H_3O^+ (proton) shuttle is facilitated by the imidazole group of His_{64} (Fig. 1A) and unbranched networks mediated by two or three water molecules at the active site facilitate the proton transfer when His_{64} is present in its inward conformation (see Fig. 1A) [7]. Site-directed mutagenesis studies on several mutants of CA II clearly indicate the important role of His_{64} on the overall rate of catalysis [4,7]. It is intriguing to note that in spite of a reduced catalytic efficiency, the activity of the enzyme is not completely lost.

The proton transfer pathways that relay the excess charge over several molecular diameters may be modeled as hydrogen-bound networks formed by polar side chains (His, Glu and Thr, see Fig. 1A) and water molecules [8], present in a "proton channel" of the protein, which may be used in proposing the mechanism of proton transfer into the active site. According to the Grotthuss-like mechanism [9,10], a proton transfer process consists of two elementary steps; (I) hopping of the proton between donor and acceptor sites and (II) turn or reorientation to optimize the donor–acceptor distance for an effective hopping (see "in"/"out" positions of His_{64} in Fig. 1A). Additionally, the proton transfer step (as the rate limiting step of CA catalysis) itself may encounter a large free energy barrier and thus become slow [10]. Thr_{199}, together with Thr_{200}, is involved in a finely tuned network of hydrogen bonds (as a second coordination sphere) leading toward the solvent-exposed His_{64}, which is located at the entrance of the active-site channel and has a critical role with the help of a cluster of histidine residues (residues 3, 4, 10, 15, 17).

For a long time, it was believed that carbonic anhydrase exhibited absolute specificity, i.e. that it would only catalyze the interconversion between CO_2 and HCO_3^-. However, in the 1960s it was discovered that the enzyme also catalyzes hydration of various aldehydes as well as hydrolysis of esters [11] (see Fig. 1B). Based on the literature [11], the elements of both lyase and esterase active sites of CA are the same (compare Fig. 1A and B) so that enzymatic hydrolysis of esters appears to be either controlled by the same amino acid side chains.

According to the vital physiological roles of CAs and regarding the earlier statements, it seems plausible that modulation of CA activity to normal levels either by inhibition or activation offers interesting therapeutic options [12,13]. Blockade of CA activity in local tissues may therefore increase tissue CO_2 concentrations and/or lower tissue pH, resulting in vascular dilation and increased blood flow. On the other hand, CA can change hemoglobin's affinity for oxygen by controlling the movement of CO_2 gas between air and liquid compartments. Deficiency of hCA is the primary defect in the syndrome of osteopetrosis, renal tubular acidosis, and cerebral calcification [14]. Unlike CA inhibitors, widely used clinically for the treatment or prevention of a multitude of diseases, CA activators have been much less investigated [15]. In the past decade, by means of X-ray crystallography, electronic spectroscopy, and kinetic measurement, it has been proved that the most activator molecules (for instance, see Structure 1) bind at the rim of enzyme active cavity, participating in the rate-determining step of the catalytic cycle [16,17]. As stated earlier, the entrance of the active site of isozyme hCA II contains a cluster of six histidine residues (His_3, His_4, His_{10}, His_{15}, His_{17} and His_{64}), some of which possess different conformations (as shown by X-ray crystallography) which could easily participate in interaction with the activator molecules [18]. Furthermore, regarding the binding site of various activators, it appears that they induce a finely tuned network of hydrogen bonds both in and at the rim of enzyme active site facilitating proton shuttling from solvent to the catalytic site and vice versa [4].

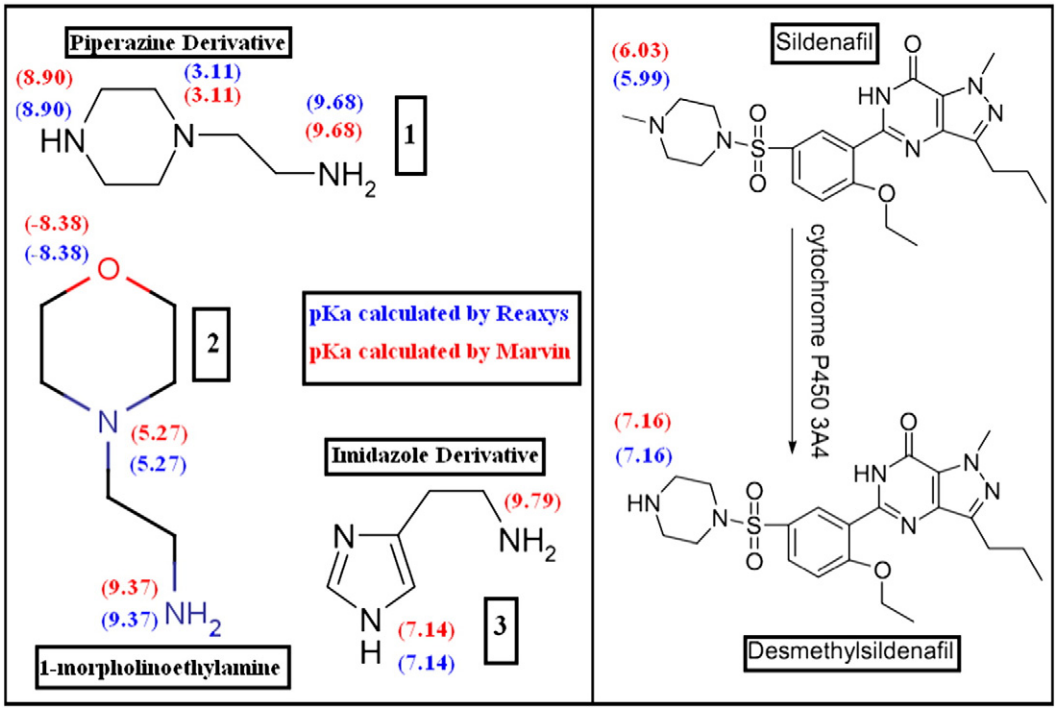

Structure 1. (right) Structure of 1-[4-ethoxy-3-(6,7-dihydro-1-methyl-7-oxo-3-propyl-1H-pyrazolo[4,3-d] pyrimidin-5-yl) phenylsulfonyl]-4-methylpiperazine (Sildenafil) and Metabolic transformation of it to the desmethylated compound [19]. (Left) Calculated pKa values of imidazole (3), piperazine (1) and morpholine (2) derivatives [15] using Reaxys (http://www.reaxys.com) as well as with the ChemAxon's Marvin plug-in calculator (<http://www.chemaxon.com/marvin>).

Sildenafil (1-[4-ethoxy-3-(6,7-dihydro-1-methyl-7-oxo-3-propyl-1*H*-pyrazolo[4,3*d*]pyrimidin-5-yl) phenylsulfonyl]-4-methylpiperazine, Structure 1), a phosphodiesterase-5 (PDE5) inhibitor, is a widely used drug for the treatment of erectile dysfunction (ED) [19]. The pharmacological role of this drug is to prolong the signaling actions of nitric oxide (NO) in penile smooth [20] and through reducing the degradation of cGMP, allowing erectile function to occur by relaxation of penile smooth muscle. Interaction of sildenafil with other zinc-enzymes than the PDEs has been very rare in the literature to date (except for Supuran et al. [19]), although there are many zinc-enzymes (e.g. CA) in mammals that might interfere with sildenafil. There are also no reports regarding the mechanistic details of CA–sildenafil interaction. Therefore, we decided to investigate the interaction of this drug, which does not possess any of the common pharmacophores present in the CA inhibitors (CAIs) but it has the piperazine moiety present in some CA activators [20,21], with CA II isoenzyme (see Structure 1). In the present research, we analyzed the interaction of sildenafil with native and histidine-modified hCA II using UV–vis, circular dichroism (CD) and fluorescence spectroscopic techniques. In this study, we further characterized the mode/strength of drug binding, the related thermodynamic parameters and structural/functional alterations of hCA II upon the binding process. Moreover, using histidine modification with diethyl pyrocarbonate (DEPC), we proposed that piperazine moiety of the drug (as an external member of the cluster of H^+ donor/acceptors existing at the rim of CA active site) can restore enzyme catalytic ability via interfering in the proton transferring process.

2. Materials and methods

2.1. Chemicals

The *p*-nitrophenyl acetate (*p*-NPA) and 1-anilinonaphtalene-8-sulfonate (ANS) were purchased from Sigma Chemical Co (St. Louis, Mo, USA). Diethyl pyrocarbonate (DEPC) was obtained from Fluka. Pure sildenafil was obtained as a generous gift from Fertility and Infertility Research Center (Kermanshah, Iran). The other reagents were of analytical grade and used as obtained from the suppliers. All the solutions were prepared in double distilled water and, unless stated otherwise, all experiments were carried out in 50 mM sodium phosphate, pH 7.0 as the buffer utilizing double distilled water with very low conductivity, at room temperature. Enzyme concentration was estimated by measuring the absorbance at 280 nm ($\varepsilon_{280} = 54{,}000\ M^{-1}\ cm^{-1}$) [17]. CD experiments were carried out in 50 mM Tris–HCl, pH 7. The pK_a value for the nitrogens of CA activators and piperazine moiety of N-desmethyl sildenafil calculated by Reaxys (http://www.reaxys.com) as well as with the ChemAxon's Marvin plug-in calculator (http://www.chemaxon.com/marvin).

2.2. Protein purification

Human CA II was purified from human erythrocytes according to the method described by Nyman [22]. SDS-polyacrylamide gel electrophoresis was used to confirm the protein purity. The concentration of hCA was determined according to Lowry's method [23] and standard curve was generated using BSA.

2.3. Enzyme assay

Carbonic anhydrase assays (colorimetric assay for esterase activity) were performed at 25 °C according to Pocker's method [24]. The enzyme-catalyzed reaction was followed at 400 nm using a Cary Eclipse (Varian) UV–vis spectrophotometer in quartz cells with 1 cm wavelength. Stock solution of *p*NPAc (138 mM) was prepared by dissolving 0.050 g of *p*NPAc in 2.0 ml of acetonitrile. The different *p*NPAc concentrations were applied for the determination of the kinetic parameters. The activator and enzyme solutions were preincubated together for 15 min, prior to assay, in order to allow for the formation of the enzyme–activator complex. The final enzyme concentration in the assay buffer was 2.0 μM. It is noteworthy that sildenafil had no effect on the rate of non-enzymatic degradation of *p*NPAc.

2.4. Modification of hystidine residues

Diethylpyrocarbonate (DEPC) was used to (specifically) modify histidines in the CA II. Stock solution of 0.1 M DEPC in absolute ethanol was prepared and the final ethanol concentration did not exceed 1% by volume. Freshly prepared DEPC solution was added to the protein [25] to obtain a protein:DEPC molar ratio in the range of 1:1 to 1:900. The reaction tubes were incubated at 4 °C. After incubation, protein samples were dialyzed extensively against 50 mM phosphate buffer, pH 7 (in the pH range of 5.5 to 7.5, DEPC is reasonably specific for reaction with histidyl residues) overnight at 4 °C, so excess DEPC was removed [25]. The concentration of the modified protein was also determined according to Lowry's method.

The number of modified histidyl residues was calculated from the following equation:

$$\frac{(0.8\ \text{ml/ml of test solution}) \times A_{240} \times MW}{(\text{mg of protein/ml of test solution}) \times \Delta\varepsilon}. \quad (1)$$

Where $\Delta\varepsilon$ is the molar extinction coefficient of modified histidine residues ($3200\ M^{-1}\ cm^{-1}$), MW is the molecular mass of hCA II (29 kDa) and A_{240} is the absorbance at 240 nm [26].

2.5. Circular dichroism (CD) spectroscopy

The CD spectra were obtained by a JASCO-810 spectropolarimeter, using a 1 mm pathlength cell in 50 mM Tris–HCl buffer, pH 7.0. The spectra were recorded in the range of 190–250 nm and 250–350 nm for far- and near-UV CD, respectively. The CD spectrum of hCA II (0.3 and 1.3 mg/ml for far- and near-UV CD, respectively) were recorded in the absence and presence of 100 and 150 μM sildenafil. The data were normally plotted as mean residue ellipticity (MRE, $degree \cdot cm^2 \cdot dmol^{-1}$) versus wavelength in nm, calculated via following equation:

$$MRE = \text{observed CD(mdeg)}/C_P nl \times 10 \quad (2)$$

where Cp is the molar concentration of the protein, *n* is the number of amino acid residues, and *l* is the path length [27]. The α-helical contents of native and modified hCA II and in the absence and presence of sildenafil were calculated from MRE values at 208 nm using the equation:

$$\alpha - Helix\ (\%) = \{(-[MRE]_{208} - 4000)/(33{,}000 - 4000)\} \times 100 \quad (3)$$

where MRE_{208} is the observed MRE value at 208 nm, 4000 is the MRE of the β-form and random coil conformation cross at 208 nm and 33,000 is the MRE value of a pure α-helix at 208 nm. From the above equation, the α-helicity in the secondary structure of the native and modified hCA II was determined [28,29].

2.6. Fluorescence spectroscopy

Fluorescence measurements were made on a Cary Eclipse (Varian) fluorometer with jacketed cell holder in which temperature was adjusted by an external thermostated water circulation. Excitation was at 295 nm and the spectral bandwidths of both the excitation and emission slits were set to 5 nm.

The fluorescence data was corrected for inner filter effect using the equation:

$$F_{corr} = (F_{obs}) \times Anti\log \times \left(\frac{A_{exc.} + A_{em.}}{2}\right) \quad (4)$$

where and are the observed and corrected fluorescence intensities, and $A_{exc.}$ and $A_{em.}$ are the absorbances at excitation and emission wavelengths, respectively [30].

2.6.1. ANS fluorescence and determination of PSH

Changes in PSH can be monitored by the probe 1-anilinonaphtalen-8-sulfonate (ANS) [31,32]. Titration of enzyme solutions in the presence of increasing concentrations of ANS provide information about difference in the ANS binding properties of native and modified hCA II by determining the F_{max} and K_d^{app} of the enzyme-ANS complexes, in the absence and presence of sildenafil [32]. F_{max} is the maximum fluorescence intensity at the saturated ANS concentration which indicates the number of surface hydrophobic sites of the protein. K_d^{app} is the apparent dissociation constant for ANS. The assay solutions (0.3 mg/ml protein in the presence of various concentrations of ANS) were excited at 380 nm and emissions were recorded over range 400–600 nm [31,32]. ANS was added from a stock solution (1 mM) to the final concentration range from 2 to 120 μM. The increase in fluorescence emission was recorded until no further increase in fluorescence was observed. The protein surface hydrophobicity of native and modified hCA II, free and complexed with sildenafil can be calculated from the following equation [32]:

$$PSH = F_{max}/[\text{hCA II}]K_d^{app} \quad (5)$$

2.6.2. Fluorescence quenching

Fluorescence quenching is a valuable method for studying the interaction of substances with protein. The quenching process can be induced by a collisional process or a formation of a complex between quencher and fluorophore. The former is referred to as a dynamic quenching mechanism and the latter a static quenching mechanism. Solute quenching experiments were carried out by the addition of aliquots of concentrated stock solutions of sildenafil to the protein solutions (0.02 mg/ml) which were incubated at 25, 30, 35 and 40 °C. The emission spectra were recorded in the range of 310–400 nm at the excitation wavelength of 295 nm. The data herein obtained were analyzed by the Stern–Volmer equation [33]:

$$F_0/F = 1 + K_{SV}[Q] \quad (6)$$

where [Q] is the molar concentration of quencher, K_{sv} is the Stern–Volmer quenching constant, F_0 and F are the fluorescence intensities in the absence and the presence of quencher.

The number of binding sites and the value of association constant (K_b) were estimated by fitting the experimental data to the modified Stern–Volmer equation:

$$\log\{(F_0 - F)/F\} = \log K_b + n\log[Q] \quad (7)$$

where K_b and n are the association constant and the number of binding sites, respectively. The values of n and K_b were obtained from the slope and Y-intercept of the modified Stern–Volmer plot, respectively [34].

2.6.3. Calculation of thermodynamic parameters

The thermodynamic parameters, enthalpy changes (ΔH°), entropy changes (ΔS°) and free energy changes (ΔG°) are the main evidences to determine the binding mode. The thermodynamic parameters were estimated by van't Hoff equation:

$$\ln K_b = -\Delta H^\circ/RT + \Delta S^\circ/R \quad (8)$$

where K and R are the binding constant and universal gas constant, respectively, afterward the free energy change ΔG° can also be evaluated by the Gibbs equation [35]:

$$\Delta G^\circ = \Delta H^\circ - T\Delta S^\circ. \quad (9)$$

2.7. Particle size measurements using dynamic light scattering (DLS)

Measurement of the apparent hydrodynamic diameters of the native and modified hCA II was accomplished using photon correlation spectroscopy. Samples were prepared as described in far-UV CD section at a protein concentration of 0.17 mg/ml. The concentration of the protein stock solution was measured immediately before sample preparation, after the stock was filtered with a 20-nm syringe filter (Whatman, Maidstone, UK). Buffer solutions were also filtered. The DLS measurements were performed at 25 °C using a Malvern Zetasizer Nano S instrument (Malvern, Worcestershire, UK) equipped with a Peltier temperature controller. Disposable polystyrene cuvettes having a 1-cm path length were used. Every sample was measured six times and the average distributions are reported. The average and the standard deviation values of the sizes corresponding to the peak of interest in each of these six distributions provide the apparent hydrodynamic diameter and the experimental error for each sample.

2.8. UV absorbance measurements

The UV absorbance spectra were recorded on a UV–vis spectrophotometer Cary Eclipse (Varian) equipped with 1 cm quartz cells. In this experiment, native and modified hCA II concentrations were fixed at 0.1 mg/ml while the drug concentration was varied.

2.9. Computer simulation studies

2.9.1. Theoretical modification and docking studies

The crystal structure of native hCA II (PDB 3KS3) was downloaded from the protein data bank (PDB) (www.pdb.org). We chose histidine surface residues, which have > 30% accessible surface area assessed in Swiss-PDB Viewer (version 4.0.1) [36]. The atomic coordinates of sildenafil was built using Hyperchem program (version 8.0) in PDB format [37]. Imidazole side chains of histidine residues 4, 10, and 36 of CA were modified (see Fig. 2A) to generate the initial structure of the modified enzyme. The native and modified proteins were selected for docking process to study the sildenafil interaction. The optimized structure of the ligand was used as input of Auto Dock Tools and the partial charges of atoms were calculated using Gasteiger–Marsili procedure. Using AutoGrid tools, the grid maps were generated adequately large to include the active site of protein as well as significant regions of the surrounding surface. In all cases, a grid of $100 \times 82 \times 90$ points in the x-, y-, and z-axis directions and a grid spacing of 0.397 Å was applied in each Cartesian direction. Then, the most suitable structure for the flexible ligand molecule was optimized by the rotation of all single bonds in the ligand molecule. The grid parameter file and the docking parameter file were set up by the AutoDock Tools program. Population size was 256 and a maximum number of 2,000,000 for energy evaluations was used. Default settings were used for all other parameters. Docking calculations were carried out with the rigid native and modified hCA II, and a flexible ligand [38] using a Lamarckian genetic algorithm [39]. The most suitable conformations of native- or modified-CA, in terms of energy and cluster population, were selected for molecular dynamics studying. Molecular graphics were prepared by VMD version 1.8.9 [40].

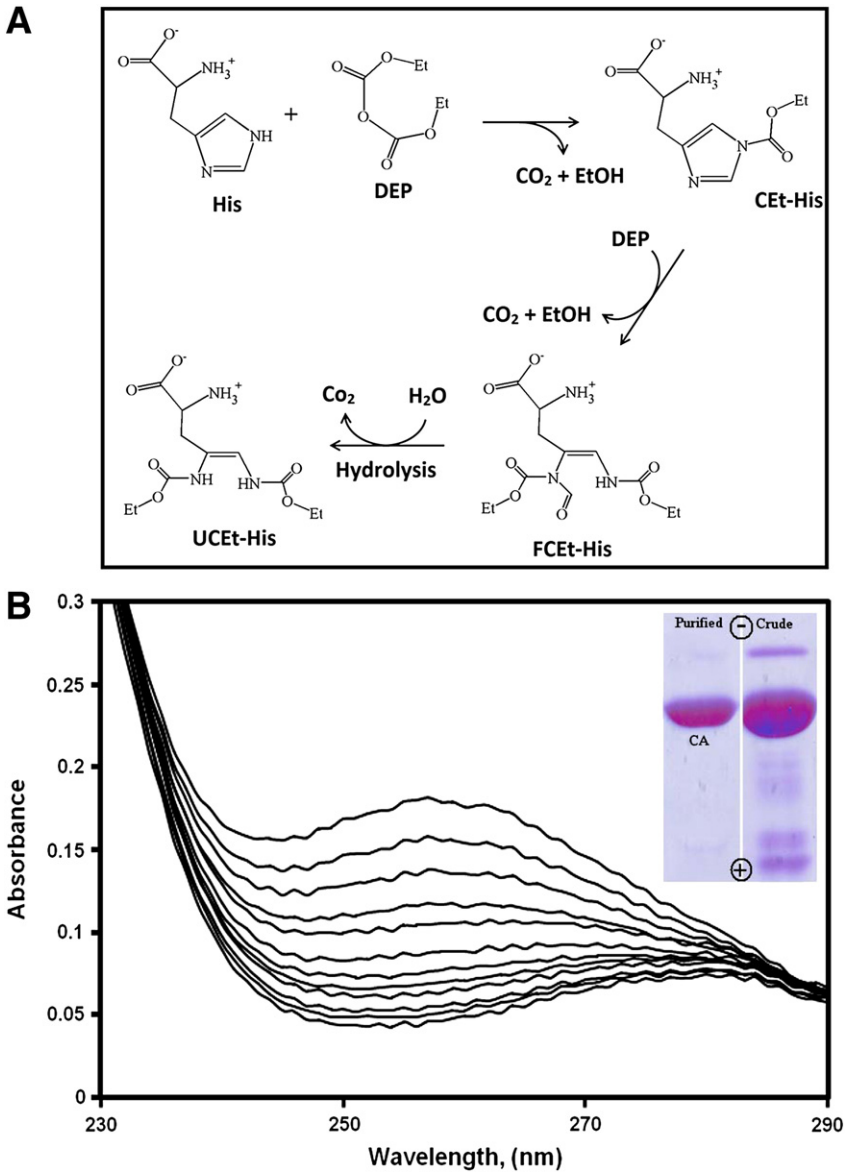

Fig. 2. (A) Modified form of histidine residue after interaction with DEPC (DEP), reproduced from [25,26]. CEt (Carbethoxy), FCEt (Formyl-biscarbethoxy), UCEt (Urethane-carbethoxy). (B) UV absorbance spectra of hCA in the presence of DEPC ([protein]:[DEPC] molar ratios were in the range of 1:1 to 1:900). All data shown are representative of three independent experiments. (Inset) SDS-PAGE of the purified and crude CA samples. For more details please see experimental procedures.

2.10. Molecular dynamics simulations

All MD simulations were carried out using the GROMACS simulation package [41], version 4.5.5 with GROMACS force field, on an Intel Core i7 Extreme Edition under Red Hat Enterprise Linux 5.0. The starting atomic coordinate of CA was obtained from Protein Data Bank (PDB) code 3KS3 [42]. The GROMACS topology and parameter files of sildenafil and modified side chains of histidine residues were generated using PRODRG web server [43]. Each protein, native CA, modified CA or CA–sildenafil complex was centered in a cubic box and then solvated with water molecules. Counterions Cl^- and Na^+ were added by replacing water molecules at random positions to achieve a neutral simulation box. The solvated and neutralized systems were subjected to energy minimization until the maximum forces were smaller than 500. In all simulations, the temperature was kept close to 300 K by the Berendsen algorithm [44] with $\tau_T = 0.1$ ps and pressure was kept close to 1 bar by the Parrinello–Rahman algorithm [45], with $\tau_P = 2$ ps. Bond lengths were constrained using the LINCS algorithm [46,47]. Lennard–Jones and short-range electrostatic interactions were calculated with 1.4- and 0.9-nm cutoffs, respectively, and a particle mesh Ewald algorithm was used for the long-range electrostatic interactions [48]. The neighbor list was updated every 2 steps. Each component of the system was coupled separately to a thermal bath, and isotropic pressure coupling was used to keep the pressure at the desired value. A time step of 2 fs was used for the integration of the equation of motion. To relax the solvent molecules, a 100-ps position-restrained MD simulation was preformed to equilibrate the system. Then, a 100-ps or 200-ps equilibration under NpT ensemble was applied. Finally, the production MD periods of 20 ns or 40 ns at constant pressure and temperature was performed on both of the modified and native CA, respectively.

3. Results and discussion

The CAs are involved in a multitude of physiological or pathological processes such as biosynthetic reactions, respiration, ionic transport, secretion of electrolytes, acid–base regulation, pH homeostasis,

calcification and tumorigenicity. Modulation of enzyme activity by means of activators and inhibitors constitutes an important pharmacologic tool for the management of several pathologies. Among the several CA activators, histamine and piperazine derivatives have been investigated in detail [4,15,19]. Several kinetic as well as X-ray crystallographic studies revealed that most CA activators bind at the entrance of the active site cavity of the enzyme, in a region different from the inhibitor/substrate binding site and to facilitate the rate-determining step of the catalytic turnover, that is the transfer of a proton from the zinc-bound water molecule to the environment.

In different CA isozymes, His_{64} or a histidine cluster (His residues 3, 4, 10, 15 and 64, in the case of CAII) assists the proton transfer process [7]. Modification of involved histidine residues may give critical information in this area. Diethylpyrocarbonate (DEPC), at a certain pH range, is the most extensively used reagent for the specific modification of histidine in proteins [25,26]. After hCA purification (Fig. 2, inset), modification of enzyme's histidine residues (Fig. 2A) at a moderate excess of DEPC was performed. This type of modification results in substitution at one of the nitrogen positions on the accessible imidazole moieties [25]. Human CA II has 11 histidine residues which account for a small part of the 260 total residues of hCA II, 3 of which are surface exposed.

The reaction between DEPC and histidine is accompanied by an increase in absorbance at 240 nm (Fig. 2B) [25,26]. The changes in absorption spectrum of hCA II during modification with DEPC (protein: DEPC molar ratio in the range of 1:1 to 1:900) showed an increase at the 230–250 nm range. The number of modified residues was calculated (Eq. (1)) by using 3200 $M^{-1}\cdot cm^{-1}$ as the molar absorption coefficient for modified histidines [28]. When [DEPC] was applied at mild concentration, the result showed that 3–5 histidine residues were modified. It is noteworthy that an accessible histidine residue will have a relatively fast modification rate with DEPC, whereas a buried residue will have a relatively slow modification rate. His_{64}, for instance, has been found to be buried even when its side chain is present in an outward conformation. In this way, only accessible histidine residues (including His_4 and His_{10}), which have >30% accessible surface areas, assessed in Swiss-PDB Viewer, were proposed to be the more susceptible sites in experimental modification and also were considered for in silico manipulation [36]. It should be noted that, based on calculated pK_a values (>10), nitrogen atoms of the amine groups in modified histidines (Fig. 2) cannot be protonated at pH values in the physiological range so that these modified side chains may not efficiently act as members of the proton shuttle system.

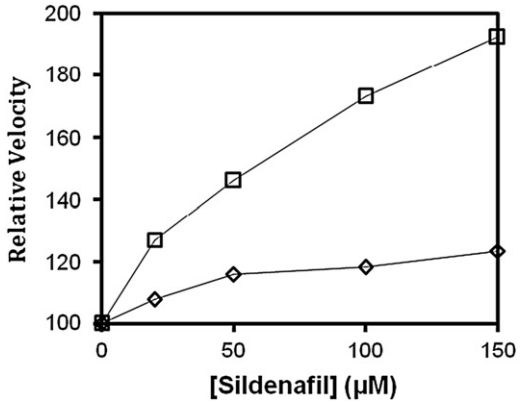

Fig. 3. Velocity measurements of native (◊) and modified (□) hCA II in the presence of sildenafil. All data shown are representative of three independent experiments. Changes in enzyme activities were normalized according to the activity in the absence of the drug. For more details, please see experimental procedures.

3.1. Esterase activity of native and modified human carbonic anhydrase II

The promiscuous esterase activity of CA probably stems from the mechanistic similarity between hydration of the carbonyl of CO_2 and that of an ester (see also Fig. 1). Indeed the steric and electronic natures of CO_2, *p*NPAc and the respective intermediates and transition states are significantly different, so that all catalytic events (including H^+ transfer) in esterase activity become slow and finally the rate of promiscuous hydrolysis of pNPAc is ~10^5 fold less than the rate of CO_2 hydration. It has been also reported that the esterase activity proceeds through an acyl-enzyme intermediate [49]. Additionally, contrary to lyase/hydratase activity of CA, little is known about the rate limiting step (RLS) of its esterase activity and there is a discrepancy whether it is limited by the rate of hydroxide ion attack, H^+ transfer rate or acyl group departure [49,50]. If we assume that the RLS of both hydratase and esterase activities of CA is the same step, then there is also this possibility that enzyme esterase activity decreases when manipulating the histidine members of the H^+ shuttling system and that the suppressed activity may be revived by introducing an activator such as sildenafil.

We observed a relative decrease (~60%) in the rate of catalytic turnover upon DEPC-mediated chemical modification of CA, in the absence of sildenafil. Thus, it may be concluded that only some ancillary (and exposed) imidazole side chains of histidine cluster (such as His_4 and His_{10} but not essential His_{64}) have been changed resulting from partial disturbance in proton transfer pathways (see modified His residues in Fig. 4B). The CA activity may be restored by sildenafil. In this way, esterase activity of native and modified enzyme was assayed based on *p*-NPA hydrolysis in the presence of sildenafil. The initial velocity (V) was determined as the slope of the absorbance changes at 400 nm during the linear phase of the catalytic reaction [51], so that sildenafil was evaluated as an activator of native and modified hCA II. The results showed that catalytic activity of native CAII increased under the effect of sildenafil, so that the slope of the respective curve (enzyme esterase activity versus [drug]) increased slightly with an increase in sildenafil concentration (Fig. 3). Additionally, a dramatic enhancement of modified CA activity was observed, confirming that the rescue of CAII-sildenafil seems to depend on specific interaction between enzyme and H^+ donor/acceptor part of the drug that helps interamolecular H^+ shuttle (catalytic activity) and H^+ exchange between the catalytic center and the surrounding solvent. Regarding the activator's binding site, sildenafil may provide an efficient supplementary proton release pathway especially in the modified enzyme–sildenafil complex. In this regard, the addition of certain buffers such as imidazole and carnosine (as efficient H^+ donor/acceptors) has been also observed to restore the enzyme's lyase activity in vitro [4,19].

The results of enzyme assays (Fig. 3) are in accordance with the computer simulation studies. First, using the known X-ray crystallographic structure of the human carbonic anhydrase II (PDB code 3KS3), two 3D models of the enzyme were constructed differing in the residues His_4, His_{10}, and His_{36}. To conserve the original amino acid patterns of the X-ray structure, the control model (native hCA II), was constructed with these residues to be histidines in their non-cationic forms and in the modified model, side chains of His_4, His_{10}, and His_{36} were replaced by the modified moiety (Fig. 4). It has been proven that the activators bind at the entrance of the active site cavity, in regions different from the inhibitor or substrate binding sites, and to participate the rate-determining step of the catalytic cycle [10,52]. Docking and MD studies (Fig. 4A) suggest that sildenafil and substrate/inhibitor binding sites on both the native and modified CA molecules are also not the same. Fig. 4 also presents the magnified segments of the enzyme indicating that the sildenafil binding site as well as the location of the side chains of the "histidine cluster" change slightly upon modification, so that the piperazine moiety of the drug (metabolite), at the entrance of the active site cavity, in close vicinity of the natural proton shuttle of hCA II (i.e., His_{64}) and the cluster of histidines, may affect existing shuttling system or contribute to a supplementary proton release pathway

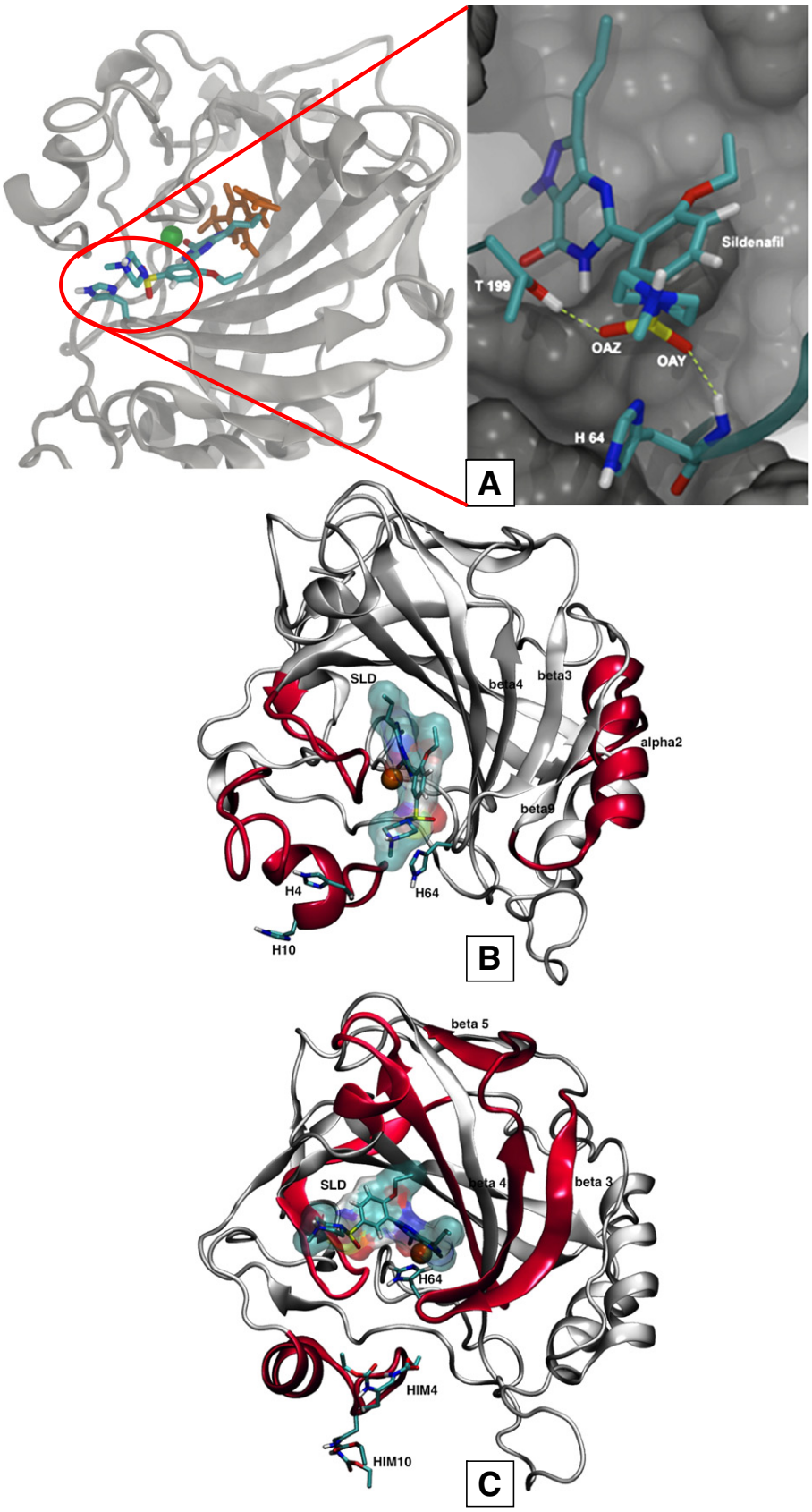

Fig. 4. (A) Different binding sites of sildenafil (represented as CPK) and a CA inhibitor (furosemide, orange molecule) on hCA II. Pay attention to the vicinity of sildenafil piperazine moiety and His-64 and also to hydrogen-bonding between oxygen atoms of sildenafil (OAY and OAZ) and NH backbone of His-64 and hydroxyl group of Thr-199. Green sphere is considered as the catalytic zinc ion. (B, C) 3D representation of the MD average structure of the native (B) and modified (C) hCA II in complex with sildenafil. Accessible histidine residues (H_4 and H_{10}) in the native enzyme that are prone to modification and their modified counterpart (HIM) residues in the modified hCA II are shown in stick representation. Red areas in both proteins are regions that became more rigid than activator-free proteins, upon ligand binding (see next figures). Drug is also shown by CPK representation, drawn by VMD [40].

in the native CA. Furthermore, swift activity in the modified CA II, in the presence of increasing concentrations of sildenafil, may reminiscent of the formation of an alternate/efficient compensatory proton trolley (shuttle).

The backbone root mean-square deviations (RMSD) of the structures of unmodified (native) and modified CA relative to their own starting structures were 2.4 ± 0.2 Å and 2.5 ± 0.3 Å, respectively. These low RMSD values indicate that the MD runs were stable and the protein atoms did not significantly deviate from the starting structures during the MD simulations. The backbone RMSD also reflects the dynamics of the protein matrix. Average RMSD of the modified CA is higher than that of the native CA and indicates an increased flexibility of the protein backbone as a result of protein modification. To provide a more detailed description of the mobility of the protein residues, the backbone RMSD per residue (RMSF) for the native CA and native CA–sildenafil complex and also for the modified CA and modified CA–sildenafil complex are shown in Fig. 5A and B, respectively. The dark gray bands indicate mostly the α-helix regions and light gray bands indicate the β-strand regions of CA according to the crystallographic structure. It is clear from these representations that the overall structures of both native and modified enzymes (especially residues located in the α_2 region and Tyr-7, His-64, Thr-199 located in the active site cavity) experience sensible reduction in their mobility/flexibility upon ligand binding. However, due to different mode of interactions of sildenafil with the proteins, the regions undergoing the change in their mobility are very different in the native and modified CA (Fig. 5 and also see red regions in Fig. 4). For example, residues located in the 115–135 region (β7 and α1 and coiled region between them) of the modified CA–sildenafil complex experience sensible reduction in their mobility upon ligand binding while the same region in the native CA II–sildenafil complex is nearly changeless relative to the protein alone. The backbones of the residues located in the 55–85 region of the modified CA II (including β3, β4, β5 and coils between them in right part of Fig. 4C) have shown a sensible reduction in their mobility upon the activator binding. However, the global reduction in this region is not observed in the native CA–drug complex unlike the modified counterpart. In addition, the strand β9 (171–175 region) in the modified CA experiences an order-to-disorder transition upon sildenafil binding (Figs. 4 and 5C). As indicated in Fig. 5C, it seems that interactions between sildenafil and the certain regions in the modified CA II, particularly residues located in β3, β4, β5 and β7, are so strong that the hydrogen bond network between β3 and β9 was destroyed completely. Therefore, a conformational change is plausible upon the activator binding. Additionally, there is also the possibility that solvent accessible surface area (SAS) of the protein changes upon modification. In order to probe which region of the protein exhibits more solvent exposure, upon modification, surface accessible areas of the whole protein and segment 4–15 as well as region 30–40 (consisting histidine cluster) were computed during MD trajectory. As illustrated in Fig. 6, the surface accessible area of whole CA increased dramatically upon protein modification (67.37 ± 1.3 nm^2, for the native CA vs. 73.75 ± 1.43 nm^2, for the modified CA, Fig. 6A). Similar observations were also made in the case of the N-terminal region (segment 4-15) of the protein (8.94 ± 0.27 nm^2, for the native CA vs. 9.86 ± 0.43 nm^2, for the modified CA, Fig. 6B). These results are in agreement with PSH and dynamic light scattering data (see the following sections), indicating a significant increase of surface accessible area of the hCA II after surface histidine modifications.

As indicated earlier (Figs. 4A and 5A, B), some important residues of the binding site of the native CA, in the presence of sildenafil, have become more rigid than the corresponding residues in CA alone. Fig. 4A shows that the rigidities are mostly due to formed hydrogen bonds between certain atoms of the residues and sildenafil. For example, the oxygen atom of the ligand (OAY) has a potential for establishing hydrogen bonds with the NH backbone of the His_{64} residue. However, this immobilization has no effect on the mobility of the imidazole ring of His_{64}. Also, the backbones of Tyr_7, His_{64} and Thr_{199} residues located in the active site cavity of the modified CA–sildenafil complex became less flexible (Fig. 5B). On the other hand, some parts of the protein structure mainly in unstructured regions became more flexible upon ligand binding. From all these graphics, again it is evident that binding of sildenafil makes the overall backbone structure of the enzyme less flexible. Furthermore, distance analysis showed that average distances between the side chains of the residues located in the active site cavity of native CA–sildenafil complex (including Glu_{106}, Thr_{198}, Thr_{199}, Tyr_7, His_{64}, Asn_{62} and Asn_{67}) are reduced in comparison with analogous ones in CA alone (Fig. 5C and Table 1). Considering the role of these residues in the CA esterase catalysis (see Figs. 1 and 10), and especially His_{64} in proton shuttling, it may be suggested that reducing the distance between these residues can accelerate solvent-mediated proton transfer between the active site of CA and the bulk solution [53].

It is now apparent that at least four residues in the active site cavity with side chains more than 7 Å from the catalytic zinc (Tyr_7, Asn_{62}, Asn_{67}, and Lys_{170}) serve to finely tune the proton transfer properties of His_{64}. As discussed earlier, the anchored sildenafil, at the entrance of the active site cavity, binds at a site distinct from the inhibitor or substrate binding-sites (see Fig. 4A) and participates in an extended network of hydrogen bonds via interaction with amino acid residues present in the activator binding pocket (His_{64}, Asn_{67}, and Gln_{92}, Table 1) and with water molecules connecting it to the zinc-bound water, participating thereafter in the rate-determining step of the catalytic cycle. Also, CA activating behavior of desmethyl sildenafil, as the main metabolite of drug, may increase because it possesses a moiety able to participate in proton transfer processes, with a pK_a in the range of 6.0–8.0 U (see Structure 1). However, according to the computer simulation and thermodynamic observations and significant activating effect of activator on the modified CA, it can be concluded that the interacting side chains may change due to delicate structural changes induced by protein modification.

3.2. Circular dichroism measurement (CD)

Far-UV CD which can be used to follow protein structure, its denaturation and modification, is a valuable spectroscopic technique for studying protein–ligand interactions in a solution because all secondary structures have unique far-UV (190–250 nm) signals [21,54]. There is the possibility that the secondary structure of the native CA molecule (and catalytic function) changes upon modification as well as sildenafil binding. To evaluate this possibility, the far UV-CD spectra of native and modified forms of hCA II in the absence and the different concentrations of sildenafil were followed as shown in Fig. 7A, B. The α-helical contents were then estimated from MRE at 208 nm using Eq. (3). A relative increase in negative ellipticity of the "native hCA II–sildenafil" complex (attributed to enhanced helicity) was observed with an increase of drug concentration. Reciprocally, only slight changes in the intensities of the CD band (208 nm) were documented for the modified enzyme (Fig. 7B). The calculated helical contents in the native and modified enzyme with and without sildenafil are also presented in Table 2. As shown in this table, in the absence of the drug, the enzyme underwent some structural changes upon protein modification so that its α-helical content increased (24% vs. 19%). Additionally, after addition of sildenafil, considerable helical rearrangements for the unmodified CA were observed which may offer some degree of protein rigidity for the native enzyme (Table 2). According to Fig. 3, Table 2 and Fig. 5, it may be deduced that the weak activatory effect of sildenafil on the native enzyme is due to its reduced flexibility (because of its increased helicity) upon the drug binding. There is also the possibility that hydrodynamic size, and surface hydrophobicity of the protein change upon modification. As shown earlier, SAS of the CA molecules significantly increased upon protein modification, in agreement with protein size distribution results and PSH data (Table 3).

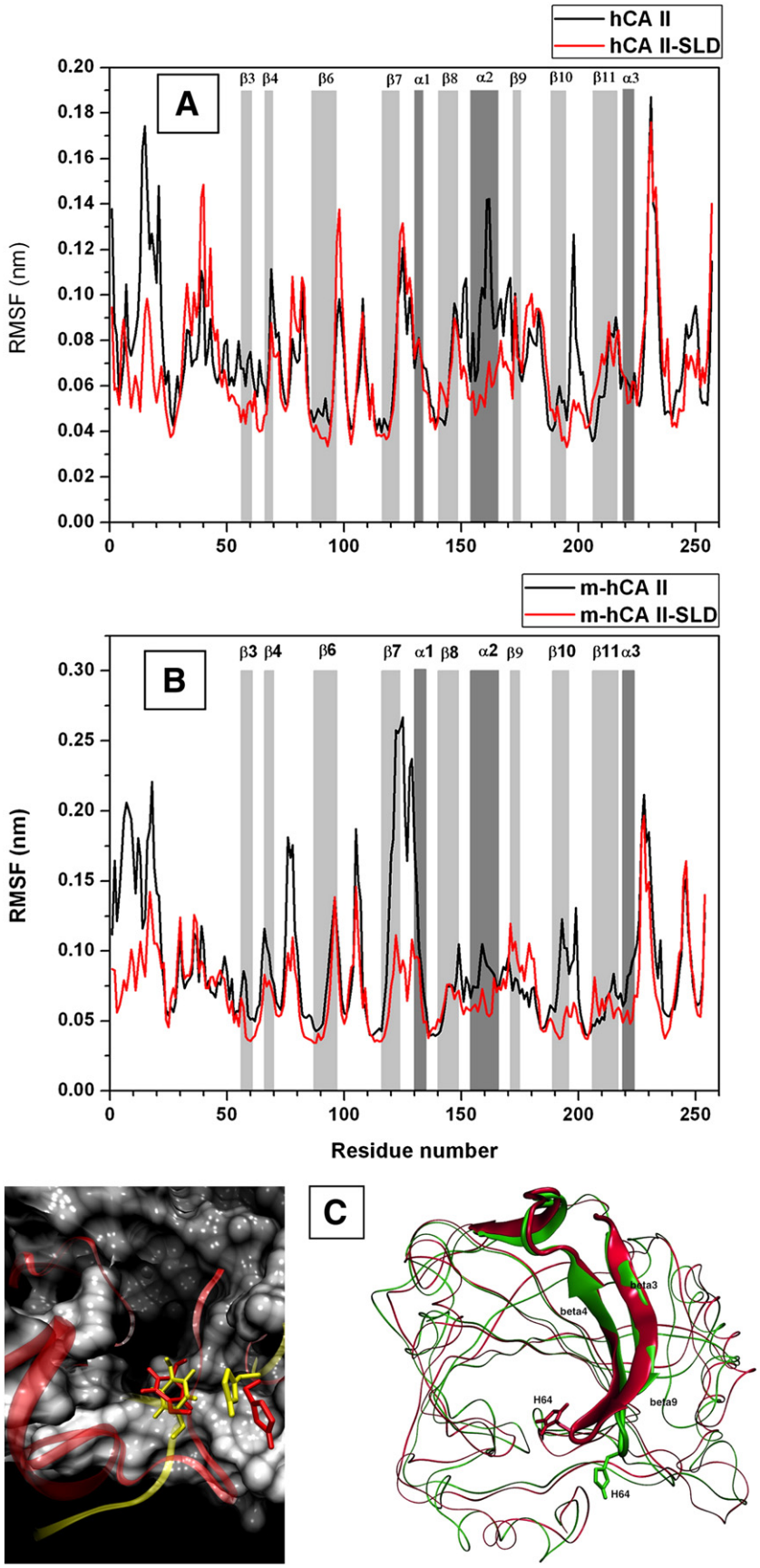

Fig. 5. The backbone atom RMSD per residue for CA alone (black lines) and CA-sildenafil complexes (red lines), for the native (A) and modified (B) enzyme. The dark gray bands indicate the helix regions and light gray bands indicate strand regions of CA II according to the crystallographic structure (PDB code: 3KS3), calculated at 300 K. (C) Right, Superimposed of the native (green) and modified (red) CA, in the presence of the activator, to illustrate ordered-to-disordered transition of strand β9, after protein modification (sildenafil has been removed for more clarity). Left, Superimposed of native CA (red) and CA–sildenafil complex (yellow) to illustrate reduced distance between His_{64} and Tyr_7 upon sildenafil binding.

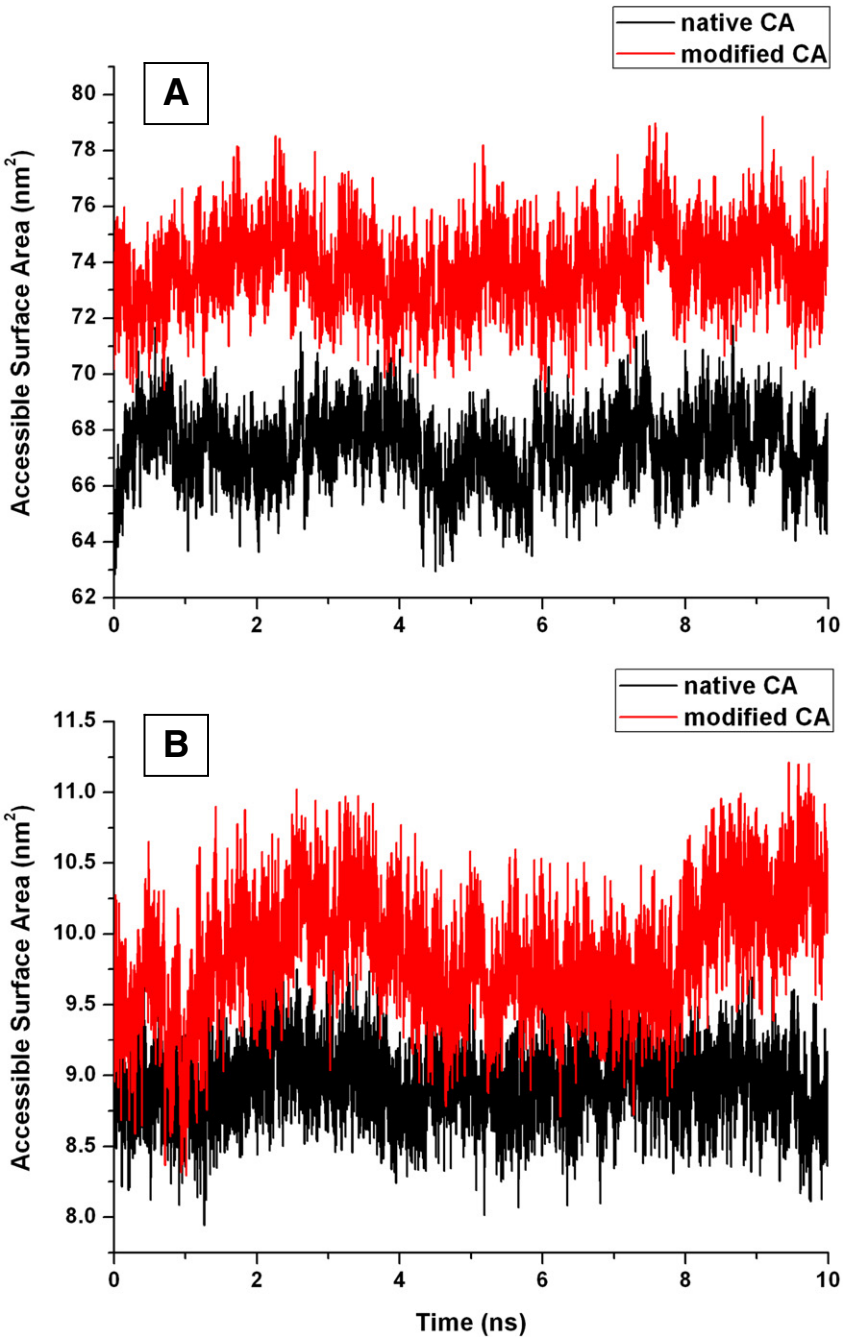

Fig. 6. Accessible surface areas of the native (black lines) and modified (red lines) protein, computed during MD trajectory, for whole CA structure (A) and its N-terminal (4–15 region) (B). See text for more details.

3.3. PSH determination induced by histidine modification in the absence and presence of the drug

There are several methods for measuring the surface hydrophobicity of proteins. ANS, as an extrinsic fluorescent probe, is extremely sensitive to polarity of the solvent. In aqueous solutions, it fluoresces very weakly, but upon binding to hydrophobic patches of proteins, its quantum yield increases significantly [55]. Thus, ANS fluorescence may be applied for monitoring possible changes in protein surface hydrophobicity induced upon drug binding. At a fixed concentration (0.3 mg/ml) of CA and increasing concentrations of ANS (0–120 μM), fluorescence intensity of ANS was measured in the absence and presence of sildenafil. By performing ANS-titration experiments, we detected differences in the ANS binding properties of hCA II in its native and modified forms. As indicated in Table 3, for both native and modified states, the ANS fluorescence in the presence of sildenafil is slightly different in comparison to the absence of the drug. Then, the values of K_d^{app} and F_{max} for the ANS were calculated from the scatchard plots [31,32]. Also, the surface hydrophobicity parameters for the native and modified protein in the absence or presence of the drug were listed in Table 3. The value of K_d^{app} for ANS binding decreased (and PSH increased) both upon protein modification and in the presence of drug, which shows the tighter binding of ANS to the modified CA and CA–drug complex. Comparing the PSH indexes of the native and modified CA (~5.3 versus ~14.4), suggests that the surface

Table 1
Average distances between important residues involved in solvent-mediated proton transfer in CA and sildenafil–CA complex.

aai–aaj	Average distance ± SD (Å)	
	CA	Sildenafil–CA complex
Y7-H64	6.8 ± 0.4	6.4 ± 0.2
Y7-T198	7.3 ± 0.3	6.7 ± 0.1
Y7-T199	7.1 ± 0.3	6.2 ± 0.1
N62-N67	7.5 ± 0.8	6.20.2
E106-T198	6.7 ± 0.1	6.6 ± 0.1

hydrophobicity of protein is increased ~200% upon modification. Increased PSH of the native (from ~5.3 to ~7.2) and modified (from ~14.4 to ~16.4) enzymes upon drug binding may also corroborate this assumption that the exact mechanism of CA activation by sildenafil may need to be reconsidered. There is the possibility that the drug exerts its activatory effects via alternative routes (such as reorganization of hydration positions and spatial rearrangement of active site elements) rather than a direct contribution to proton channeling.

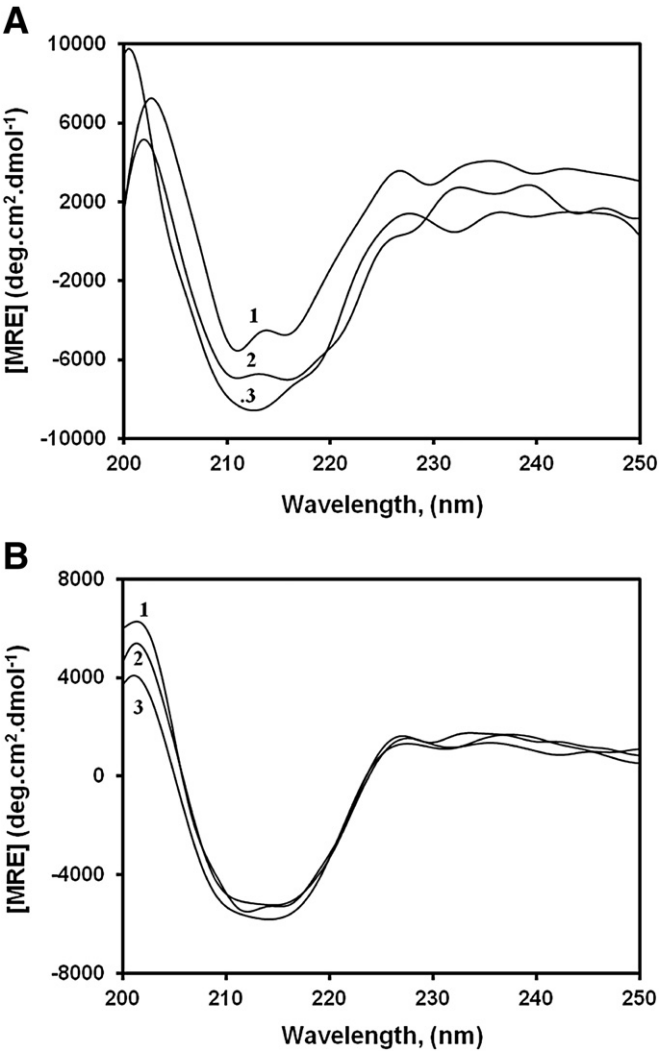

Fig. 7. The far-UV CD spectra of the native (A) and modified (B) hCA II in the absence (curve 1) and presence of 50 (curve 2) and 100 (curve 3) μM of sildenafil. The spectra were obtained in 50 mM Tris–HCl buffer, pH 7, at room temperature. Human CA II concentration was kept fixed at 0.4 mg/ml. All data shown are representative of three independent experiments. For more details please see experimental procedures.

As also indicated in Table 3, the PSH index of the modified CA changes slightly upon sildenafil binding, in full agreement with far-UV CD results (Fig. 7 and Table 2), confirming that the modified enzyme undergoes no gross structural changes, in the presence of the drug.

It is obvious that there is a linear relationship between the surface areas of amino acid residues and free energy changes associated with the transfer of the amino acids from water into the protein interior (as an oily environment) [31,32]. The degree of compactness of the protein can be quantitatively evaluated by determining the solvent accessible surface area (SAS) (see ref. [31]). As indicated in Fig. 6 and Table 3, the SAS and PSH of the CA significantly increased upon protein modification. Regarding the above statements, there is the possibility that the molecular sizes of the modified CAs increase compared to the wild-type proteins. The apparent hydrodynamic diameters of the native and modified states of CA were also measured by DLS (Fig. 8). Each sample contained only a uniform population of protein molecules with similar apparent diameter. The diameter of native protein at pH 7.0 appears to be ~5 nm. This value is consistent with the dimensions of the protein previously estimated by X-ray crystallography. As shown by Fig. 8, the protein size has increased upon chemical modification so that the hydrodynamic diameter of the modified state was found to be ~8 nm. It is logical to assume that covalently added "DEPC-derived moiety", itself, and induced conformational changes in protein structure affect molecular dimensions of CA. Overall, the analyses presented here are consistent with UV CD, ANS-derived fluorescence (and SAS) and computer simulation data indicated that the compactness of the protein decreases upon modification of accessible imidazoles especially exposed members of histidine clusters.

To come up with a correlation between the CA structural level and the (sildenafil-induced) activation of the enzyme, we evaluated the tertiary structural variation of both native and modified CAs under various drug concentrations. Fig. 9 shows the near-UV CD analyses of the native and the modified enzyme. As it is evident, histidine modification caused a change in CA CD signal in the near-UV region. The drug also caused a weak decrease in the ellipticity in both native and modified CAs which has been attributed to a minor conformational alteration in the enzyme 3D structure, upon sildenafil binding. A comparison of the CD curves with the corresponding activation profiles in Fig. 3 clearly indicates that the sildenafil-induced changes in the tertiary structure of CA have low impact on CA activation yield.

3.4. Fluorescence analyses

3.4.1. Fluorescence quenching mechanisms, determination of binding constant (K_b) and Number of binding sites (n)

HCA II consists of 260 amino acid residues forming a single polypeptide with well known sequence, which contains 7 tryptophan residues. Since many drug molecules (such as sildenafil) are fluorescence quenchers for CA, fluorescence spectroscopy became a valuable tool in the studies of drug–protein interaction. The possible quenching mechanism was interpreted by the Stern–Volmer curves and the details are listed in Table 4. A gradual decrease in the fluorescence emission intensity of the protein (increase of the F_0/F ratio, see

Table 2
Contents of α-helix in the native and modified hCA II, with and without sildenafil.

System	[Sildenafil] μM	α-Helix (%)
Native hCAII	0	19.31
	100	30.48
	150	34.06
Modified hCAII	0	24.81
	100	25.15
	150	27.72

Table 3
Surface hydrophobicity parameters for native and modified hCA II in the presence and absence of sildenafil.

Parameters	Native hCA II	Native hCA II + 150 μM sildenafil	hCA II Modified	Modified hCA II + 150 μM sildenafil
Slope ($K_A^{app} = 1/K_d^{app}$)	0.007 ± 0.012	0.012 ± 0.024	0.024 ± 0.029	0.028 ± 0.037
(F_{max}) X-interception	227.571 ± 16.161	182.083 ± 21.784	174.583 ± 2.143	170.821 ± 1.981
K_d^{app} (μM)	142.85 ± 8.53	83.33 ± 5.66	40.322 ± 1.93	34.722 ± 2.54
Ra	0.959	0.969	0.957	0.943
Surface Hydrophobicity Index (F_{max}/[hCA II] K_d^{app})	5.31 ± 0.03	7.28 ± 0.09	14.432 ± 1.65	16.411 ± 1.87

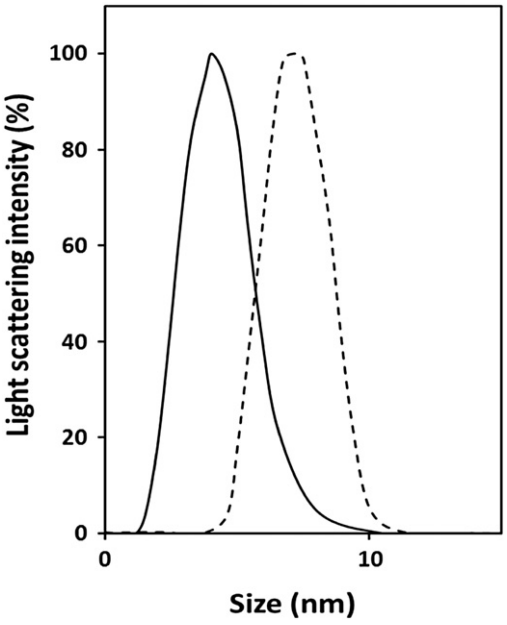

Fig. 8. Apparent hydrodynamic diameter of the native and modified CA obtained by DLS measurements. Size distributions were obtained at 25 °C in 20 mM sodium phosphate buffer plus 30 mM NaCl, pH 7. All reproduced data shown are representative of six independent experiments. For more details, please see experimental procedures.

Materials and methods section), in the presence of increasing concentrations of the drug, can be attributed to the bound drug and radiationless energy transfer between the protein tryptophan(s) and sildenafil, according to the Förster's non-radiation energy transfer theory [31]. In other words, it appears that drug binding causes fluorophores (non-polar aromatic side chains) to be more accessible to the various quenchers. These data may agree with the PSH results (Table 3). Additionally, it could be found that the Stern–Volmer plots were linear and the slops decreased with increasing temperature, which was consistent with the static type of quenching mechanism [31].

The values of sildenafil binding constant, K_b, and the number of binding sites, n, at different temperatures are also obtained by the modified Stern–Volmer plots [62] and as indicated in Table 5, the stability of "sildenafil–modified CA" complex is lower than "sildenafil–native CA" complex which surprisingly reveals the higher affinity of sildenafil for binding to the active site of native hCA II. In the case of the native enzyme, the n values at different temperatures are kept around unity, which shows the existence of one binding site in native CA. Moreover, as evidenced by Table 5, the drug–CA stoichiometries have not undergone significant changes upon protein modification. But, only at higher temperatures, n decreased.

3.4.2. Forces involved in the binding process

Essentially, there are four types of non-covalent interactions that could play a key role in drug binding to proteins including hydrogen bonds, van der Waals forces, electrostatic and hydrophobic interactions [31]. For the elucidation of the binding mode, the binding (formation) constant for Drug–CA complex formation was evaluated at four different temperatures, then the thermodynamic parameters of the binding process were obtained from van't Hoff plot (data not shown) followed by the Gibbs equation: $\Delta G^\circ = \Delta H^\circ - T\Delta S^\circ$ (Table 3). The negative values of ΔG° support the spontaneous nature of the drug binding process to the native and modified proteins. It has been accepted that when $\Delta H^\circ \leq 0$ and $\Delta S^\circ > 0$, the electrostatic force dominates the interaction; when $\Delta H^\circ < 0$ and $\Delta S^\circ < 0$, van der Waals interactions and hydrogen bonds dominate the reaction [31] and when $\Delta H^\circ > 0$ and $\Delta S^\circ > 0$, hydrophobic interactions dominate the binding process. When we apply this analysis to the binding system of drug and unmodified CA, we found that $\Delta H^\circ < 0$ and $\Delta S^\circ < 0$. Therefore, van der Waals interactions and hydrogen bonds are main forces in the binding of the investigated drug to the native CA. Additionally, the larger negative values of ΔH° and

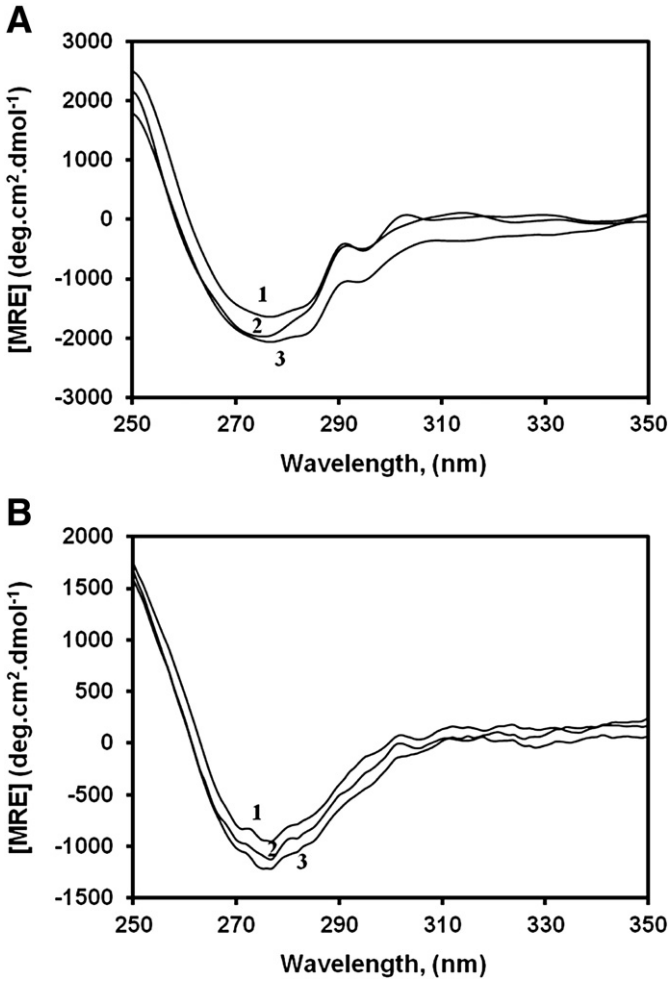

Fig. 9. The near-UV CD spectra of native (A) and modified (B) hCA II in the absence (curve 1) and the presence of 50 (curve 2) and 100 (curve 3) μM sildenafil. Final enzyme concentration was 1.3 mg/ml. All data shown are representative of three independent experiments. For more details, please see the experimental procedures.

Table 4
Thermodynamic parameters of native and modified hCA II–SIL complexes.

System	T (K)	$K_{sv}\times10^{3}$ (M^{-1})	R^2	ΔG	ΔH (kJ.mol^{-1})	ΔS (J.mol^{-1} K^{-1})
Native hCA II	298	9.13 ± 0.03	0.948	−24.54 ± 0.17		
	303	6.12 ± 0.06	0.983	−24.02 ± 0.53	−55.41 ± 3.15	
	308	4.31 ± 0.11	0.907	−23.50 ± 0.11		
	313	3.04 ± 0.02	0.952	−22.98 ± 0.92		−103.60 ± 9.58
Modified hCA II	298	6.11 ± 0.17	0.959	−23.06 ± 0.68		
	303	4.09 ± 0.25	0.905	−21.08 ± 0.08	−141.17 ± 4.72	
	308	3.73 ± 0.18	0.957	−19.10 ± 0.74		
	313	2.32 ± 0.05	0.973	−17.12 ± 0.32		−396.44 ± 6.89

Data are expressed as mean ± SD of three measurements.

Table 5
Binding parameters for the sildenafil with native and modified carbonic anhydrase at different temperatures.

System	T (K)	Binding constant $K_b\times10^{-4}$ (M^{-1})	Binding site (n)	R^2
Native hCA II	298	2.03 ± 0.531	1.085	0.958
	303	1.34 ± 0.315	1.080	0.989
	308	1.00 ± 0.037	1.111	0.913
	313	0.68 ± 0.082	1.081	0.971
Modified hCA II	298	1.17 ± 0.511	1.058	0.983
	303	0.41 ± 0.015	0.996	0.903
	308	0.17 ± 0.038	0.937	0.948
	313	0.08 ± 0.009	0.878	0.949

Data are expressed as mean ± SD of three measurements.
R^2 is the correlation coefficient for the K_b values.

$\Delta S°$ of drug binding to the modified, compared to those of the native CA, may be reminiscent of the reorganization of the hydrogen bonding network [31]. As will be discussed later, these hydrogen bonds may be employed as a part of the proton transfer network in enzyme catalysis. Overall, the above data are in agreement with the computer simulation studies (Figs. 4 and 5) indicating that the drug may bind to the modified CA to a (sub-) site rather than to its common binding site (on the wild-type enzyme). Also, the negative ΔS value suggests reorganization of hydrogen bond network which may accelerate/facilitate H^+ shuttling within modified CA active site.

Taking the above observations and also PSH results into account, there is this possibility that sildenafil activates CA (especially the modified state) via employing alternate hydrogen bond networks in the vicinity of enzyme active site (see Scheme 1). As indicated in Scheme 1, and in agreement with increased hydrodynamic size of CA after modification, since sildenafil binding to the modified CA, also, induces some minor conformational changes, the newly exposed hydrophobic side chains of aromatic/aliphatic amino acid residues, in the vicinity of active site, may have this chance to be surrounded by layers of highly ordered water molecules (increased hydrodynamic size) which may accelerate the proton transfer step (and also the rate of enzyme catalysis), only in the presence of sildenafil. In the modified enzyme, the drug binds near the 'zinc water' or H_2O_{263} (Fig. 4) which is a part of the largest hydrogen-bonded cluster A [10,12]. As partially indicated in the scheme (and Fig. 1A), there are several water molecules of which water 292 and 318 are considered to play a crucial role in forming the proton transfer path leading up to the zinc water. The drug, as the successor of the modified/exposed His_4, can act as a part of a smaller solvent exposed cluster (cluster B), comprised of His_4 and a few other (protein-bound) water

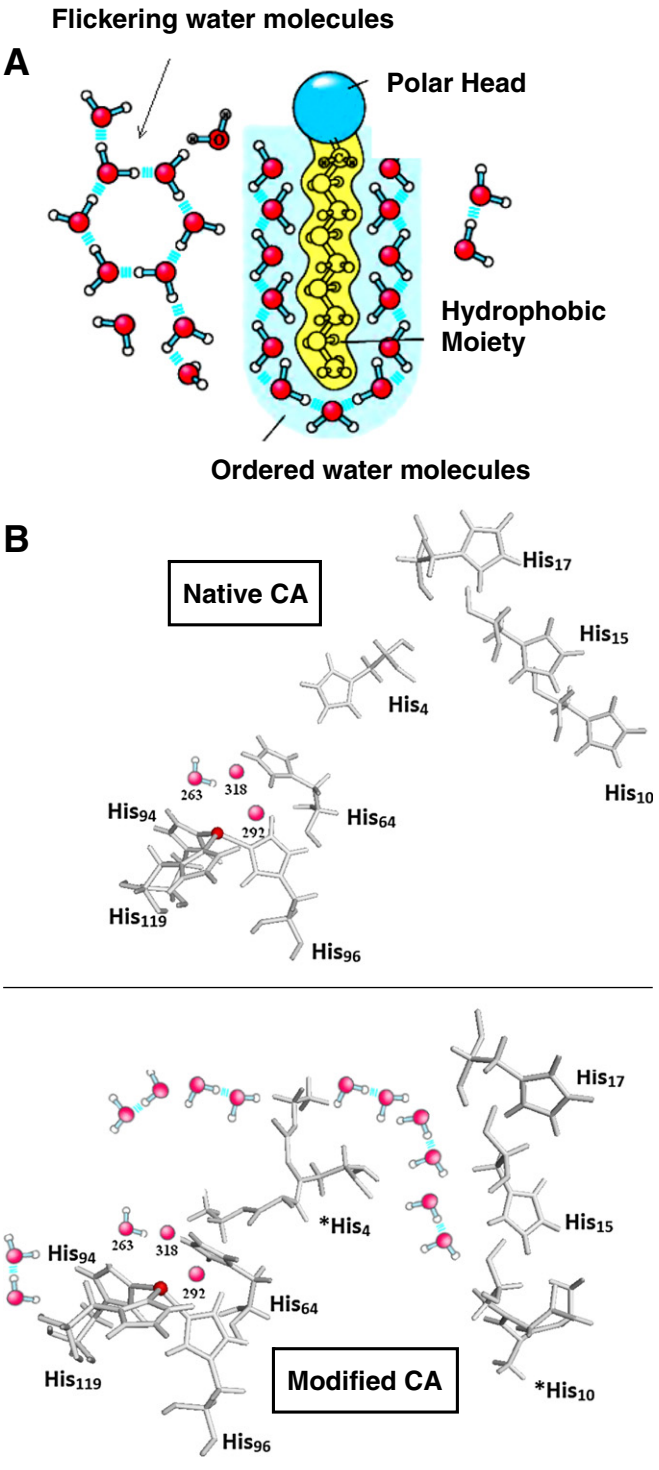

Scheme 1. (A) A proposed schematic representation of populated "protein-bound" water molecules on the hydrophobic surface of the modified CA (with higher PSH than native protein). (B) Possible contribution of sildenafil in hydrogen-bonded clusters [14] in the native (top) and modified (bottom) CA II. The selected amino acid residues are shown in stick whereas schematically added water molecules are shown in ball-and-stick representation.

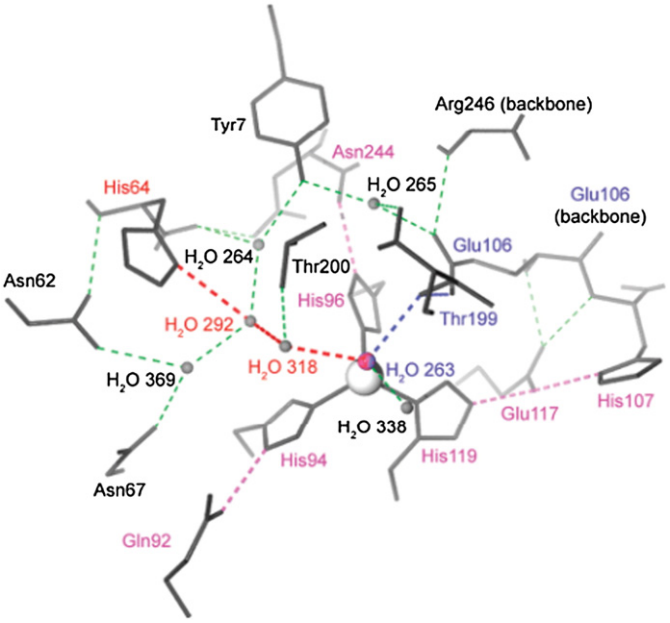

Fig. 10. The active site of HCA II in a *stick* diagram taken from ref [57]. In pink are the hydrogen bonds and residues involved in orienting the imidazole rings of His_{94}, His_{96}, and His_{119}. In blue are the residues involved in orienting the lone pairs on the zinc-bound hydroxyl ion for optimal nucleophilic attack. In red are the water molecules and His_{64}. The thin green dashed lines represent other, less crucial hydrogen bonds within the active site and further buried residues adjacent to the active site. The highly conserved residues Tyr_7, Asn_{62}, and Asn_{67} in the active-site cavity function to fine tune the properties of proton transfer by human carbonic anhydrase II.

molecules which is also extended between the active site network cluster to the protein surface.

Furthermore, it has been frequently reported that the enzyme activity is sensitive to even minor perturbations in active-site structure [10] although there is also a surprising finding in which structurally disordered "molten globule"-like structures (formed during the (un)folding of many naturally occurring enzymes) retain enzymatic function under some conditions. In addition to previously suggested mechanism for CA activation by imidazole- (or piperazine-) containing compounds, there is also the possibility that sildenafil–CA interaction affects both secondary and tertiary structures of the protein, and that the drug causes a fine structural rearrangement at the active site that leads to the formation of a high affinity "S.E" complex and more enzyme activity. Moreover, since sildenafil affects position/flexibility of the highly conserved residues Tyr_7, Asn_{62}, and Asn_{67} in the active-site cavity (Table 1, Fig. 5) which tune the properties of proton transfer of CA (Fig 10, green dashed lines), one of the possible mechanisms of sildenafil action is strengthening of less crucial hydrogen bonding networks within the CA active site.

4. Conclusion

In the present article, our aim was to study the possible mechanisms emanating from the effects of sildenafil on both proton transfer pathways and conformational fluctuations of hCA II. Modification of hCA II with DEPC resulted in the loss of enzyme activity, so it was found that decreased activity emanates from disturbance in proton transfer shuttles which is caused by modification of histidine residues. We also showed that, treatment of modified hCA II with sildenafil caused a moderate enzyme activation profile. Each CA activator must possess specific steric and electronic requirements for good activity. First, it must fit within the restricted active-site cavity of the enzyme, but should also interact favorably with amino acid residues present in the activator binding pocket. On the other hand and according to reports of Supuran [19] and Temperini et al. [56], a strong correlation has been observed between the p*K*a value of the activator molecule and its potency. Compounds with pKa in the range 6.5–8.0, for at least one deprotonatable moiety, display the best CA activating properties. Sildenafil contains an N-methylpiperazine moiety in its molecule. The pK_a value for nitrogen atom (in N-methyl group) was calculated (close to 6) using Reaxys server (http://www.reaxys.com) (Structure 1). After oral administration of the drug, it was mainly metabolized to N-desmethyl form, as the principle metabolite of the drug, through hepatic oxidation mediated by cytochrome P_{450} 3A4 (Structure 1). According to the pK_a of nitrogen atom in the metabolically modified piperazine moiety (~7, close to physiologic pH), sildenafil metabolite has more opportunity to participate in proton shuttling processes compared to the parent drug. Regarding the above statement and contrary to the suggestion in [19], we hypothesize that the CA-activating effects may be corroborated in the case of sildenafil metabolite. Furthermore, because sildenafil has a very bulky molecule, it may have difficulty binding to the CA active site. As indicated in Fig. 4A, and contrary to typical sulfonamide inhibitors, the drug was shown to be anchored at the entrance (edge) of the enzyme active site mainly by hydrogen bonding to amino acid side chains and water molecules. Sildenafil–CA interaction also leads to protein conformational changes and completes reorganization of both the hydrogen bond network within the active site cavity and hydration positions on the protein surface. Positioned in such a favorable way, it is proposed that the activator facilitates the rate-limiting step of CA catalysis, i.e., the proton transfer reaction between the zinc-bound water molecule (W_{263}) and the environment (see Eqs. (a)–(c)), which in CA II isozyme (in the absence of activators) is mainly assisted by the amino acid residue His-64 situated in the middle of the active site cavity. The pH dependence of the esterase activity of CA also strongly suggests the role of the deep water [57]. As indicated in Figs. 4A and 10 and Table 1, sildenafil may serve to finely tune the proton transfer properties of His_{64}. Additionally, as indicated in Scheme 1, the activator molecule may provide an alternative access channel to complete the proton path extended from the active site network clusters to the protein surface, thus accelerating the formation of the catalytically active nucleophilic species of the enzyme.

Acknowledgments

The financial support from the Research Council of Kermanshah University of Medical Sciences is gratefully acknowledged. We are indebted to Dr. A. A. Moosavi Movahedi (University of Tehran), Sirous Ghobadi and Dr. S. Kashanian (Razi University), for critical reading of manuscript and providing instrumental facilities as well as technical assistances.

References

[1] C.T. Supuran, A. Casini, A. Scozzafava, Protease inhibitors of the sulfonamide type: anticancer, antiinflammatory, and antiviral agents, Medicinal Research Reviews 23 (2003) 535–558.
[2] M. Imtaiyaz Hassan, B. Shajee, A. Waheed, F. Ahmad, W.S. Sly, Structure, function and applications of carbonic anhydrase isozymes, Bioorganic & Medicinal Chemistry 21 (2013) 1570–1582.
[3] A. Casini, J.Y. Winum, J.L. Montero, A. Scozzafava, C.T. Supuran, Carbonic anhydrase inhibitors: inhibition of cytosolic isozymes I and II with sulfamide derivatives, Bioorganic & Medicinal Chemistry Letters 13 (2003) 837–840.
[4] I. Elder, S. Han, C. Tu, H. Steele, P.J. Laipis, R.E. Viola, D.N. Silverman, Activation of carbonic anhydrase II by active-site incorporation of histidine analogs, Archives of Biochemistry and Biophysics 421 (2004) 283–289.
[5] C. Tu, L. Foster, A. Alvarado, R. McKenna, D.N. Silverman, S.C. Frost, Role of zinc in catalytic activity of carbonic anhydrase IX, Archives of Biochemistry and Biophysics 521 (2012) 90–94.
[6] R. Mikulski, B.S. Avvaru, C. Tu, N. Case, R. McKenna, D.N. Silverman, Kinetic and crystallographic studies of the role of tyrosine 7 in the active site of human carbonic anhydrase II, Archives of Biochemistry and Biophysics 506 (2011) 181–187.
[7] I. Elder, Z. Fisher, P.J. Laipis, C. Tu, R. McKenna, D.N. Silverman, Structural and kinetic analysis of proton shuttle residues in the active site of human carbonic anhydrase III, Proteins 68 (2007) 337–343.

[8] J.F. Domsic, W. Williams, S.Z. Fisher, C. Tu, M. Agbandje-McKenna, D.N. Silverman, R. McKenna, Structural and kinetic study of the extended active site for proton transfer in human carbonic anhydrase II, Biochemistry 49 (2010) 6394–6399.
[9] C.M. Maupin, M.G. Saunders, I.F. Thorpe, R. McKenna, D.N. Silverman, G.A. Voth, Origins of enhanced proton transport in the Y7F mutant of human carbonic anhydrase II, Journal of the American Chemical Society 130 (2008) 11399–11408.
[10] A. Roy, S. Taraphder, Role of protein motions on proton transfer pathways in human carbonic anhydrase II, Biochimica et Biophysica Acta 1804 (2010) 352–361.
[11] B. Elleby, B. Sjoblom, S. Lindskog, Changing the efficiency and specificity of the esterase activity of human carbonic anhydrase II by site-specific mutagenesis, European Journal of Biochemistry 262 (1999) 516–521.
[12] C.-C. Guoa, Y.-H. Tanga, H.-H. Hua, L.-S. Yua, J. Hui-Di, Z. Su, Analysis of chiralnon-steroidal anti-inflammatory drugs flurbiprofen, ketoprofen and etodolac binding with HSA, Journal of Pharmaceutical Analysis 1 (2011) 184–190.
[13] A. Innocenti, M.A. Firnges, J. Antel, M. Wurl, A. Scozzafava, C.T. Supuran, Carbonic anhydrase inhibitors. Inhibition of the membrane-bound human and bovine isozymes IV with sulfonamides, Bioorganic & Medicinal Chemistry Letters 15 (2005) 1149–1154.
[14] D. Lotan, A. Eisenkraft, J.M. Jacobsson, O. Bar-Yosef, R. Kleta, N. Gal, L. Raviv-Zilka, H. Gore, Y. Anikster, Clinical and molecular findings in a family with the carbonic anhydrase II deficiency syndrome, Pediatric Nephrology 21 (2006) 423–426.
[15] I. Nishimori, S. Onishi, D. Vullo, A. Innocenti, A. Scozzafava, C.T. Supuran, Carbonic anhydrase activators: the first activation study of the human secretory isoform VI with amino acids and amines, Bioorganic & Medicinal Chemistry Letters 15 (2007) 5351–5357.
[16] C. Temperini, A. Scozzafava, D. Vullo, C.T. Supuran, Carbonic anhydrase activators. Activation of isoforms I, II, IV, VA, VII, and XIV with L- and D-phenylalanine and crystallographic analysis of their adducts with isozyme II: stereospecific recognition within the active site of an enzyme and its consequences for the drug design, Journal of Medicinal Chemistry 49 (2006) 3019–3027.
[17] A. Scozzafava, C.T. Supuran, Carbonic anhydrase activators — part 21. Novel activators of isozymes I, II and IV incorporating carboxamido and ureido histamine moieties, European Journal of Medicinal Chemistry 35 (2000) 31–39.
[18] D. Hewett-Emmett, R.E. Tashian, Functional diversity, conservation, and convergence in the evolution of the alpha-, beta-, and gamma-carbonic anhydrase gene families, Molecular Phylogenetics and Evolution 5 (1996) 50–77.
[19] T. Abdulkadir Coban, S. Beydemir, I. Gulcin, D. Ekinci, A. Innocenti, D. Vullo, C.T. Supuran, Sildenafil is a strong activator of mammalian carbonic anhydrase isoforms I–XIV, Bioorganic & Medicinal Chemistry Letters 17 (2009) 5791–5795.
[20] W.D. McCubbin, C.M. Kay, S. Narindrasorasak, R. Kisilevsky, Circular-dichroism studies on two murine serum amyloid A proteins, Biochemical Journal 256 (1988) 775–783.
[21] V. Alterio, E. Langella, F. Viparelli, D. Vullo, G. Ascione, N.A. Dathan, F.M. Morel, C.T. Supuran, G. De Simone, S.M. Monti, Structural and inhibition insights into carbonic anhydrase CDCA1 from the marine diatom *Thalassiosira weissflogii*, Biochimie 94 (2012) 1232–1241.
[22] P.O. Nyman, Purification and properties of carbonic anhydrase from human erythrocytes, Biochimica et Biophysica Acta 52 (1961) 1–12.
[23] O.H. Lowry, N.J. Rosebrough, A.L. Farr, R.J. Randall, Protein measurement with the Folin phenol reagent, Journal of Biological Chemistry 193 (1951) 265–275.
[24] C.K. Tu, D.N. Silverman, Solvent deuterium isotope effects in the catalysis of oxygen-18 exchange by human carbonic anhydrase II, Biochemistry 21 (1982) 6353–6360.
[25] A. Hnizda, J. Santrucek, M. Sanda, M. Strohalm, M. Kodicek, Reactivity of histidine and lysine side-chains with diethylpyrocarbonate — a method to identify surface exposed residues in proteins, Journal of Biochemical and Biophysical Methods 70 (2008) 1091–1097.
[26] J.L. Roosemont, Reaction of histidine residues in proteins with diethylpyrocarbonate: differential molar absorptivities and reactivities, Analytical Biochemistry 88 (1978) 314–320.
[27] R.L. Mikulski, D.N. Silverman, Proton transfer in catalysis and the role of proton shuttles in carbonic anhydrase, Biochimica et Biophysica Acta 1804 (2010) 422–426.
[28] P.B. Kandagal, S. Ashoka, J. Seetharamappa, S.M. Shaikh, Y. Jadegoud, O.B. Ijare, Study of the interaction of an anticancer drug with human and bovine serum albumin: spectroscopic approach, Journal of Pharmaceutical and Biomedical Analysis 41 (2006) 393–399.
[29] X. Wu, J. Liu, Q. Wang, W. Xue, X. Yao, Y. Zhang, J. Jin, Spectroscopic and molecular modeling evidence of clozapine binding to human serum albumin at subdomain IIA, Spectrochimica Acta. Part A, Molecular and Biomolecular Spectroscopy 79 (2011) 1202–1209.
[30] N. Seedher, S. Bhatia, Mechanism of interaction of the non-steroidal antiinflammatory drugs meloxicam and nimesulide with serum albumin, Journal of Pharmaceutical and Biomedical Analysis 39 (2005) 257–262.
[31] R. Khodarahmi, S.A. Karimi, M.R. Ashrafi Kooshk, S.A. Ghadami, S. Ghobadi, M. Amani, Comparative spectroscopic studies on drug binding characteristics and protein surface hydrophobicity of native and modified forms of bovine serum albumin: possible relevance to change in protein structure/function upon non-enzymatic glycation, Spectrochimica Acta. Part A, Molecular and Biomolecular Spectroscopy 89 (2012) 177–186.
[32] S.A. Ghadami, R. Khodarahmi, S. Ghobadi, M. Ghasemi, S. Pirmoradi, Amyloid fibril formation by native and modified bovine beta-lactoglobulins proceeds through unfolded form of proteins: a comparative study, Biophysical Chemistry 159 (2011) 311–320.
[33] R. Khodarahmi, F. Naderi, A. Mostafaie, K. Mansouri, Heme, as a chaperone, binds to amyloid fibrils and forms peroxidase in vitro: possible evidence on critical role of non-specific peroxidase activity in neurodegenerative disease onset/progression using the alpha-crystallin-based experimental system, Archives of Biochemistry and Biophysics 494 (2010) 205–215.
[34] J. Chamani, A. Asoodeh, M. Homayoni-Tabrizi, Z.A. Tehranizadeh, A. Baratian, M.R. Saberi, M. Gharanfoli, Spectroscopic and nano-molecular modeling investigation on the binary and ternary bindings of colchicine and lomefloxacin to Human serum albumin with the viewpoint of multi-drug therapy, Journal of Luminescence 130 (2010) 2476–2486.
[35] P.D. Ross, S. Subramanian, Thermodynamics of protein association reactions: forces contributing to stability, Biochemistry 20 (1981) 3096–3102.
[36] N. Guex, M.C. Peitsch, SWISS-MODEL and the Swiss-PdbViewer: an environment for comparative protein modeling, Electrophoresis 18 (1997) 2714–2723.
[37] L.J. Ball, C.M. Goult, J.A. Donarski, J. Micklefield, V. Ramesh, NMR structure determination and calcium binding effects of lipopeptide antibiotic daptomycin, Organic and Biomolecular Chemistry 2 (2004) 1872–1878.
[38] G.M. Morris, D.S. Goodsell, R. Huey, A.J. Olson, Distributed automated docking of flexible ligands to proteins: parallel applications of AutoDock 2.4, Journal of Computer-Aided Molecular Design 10 (1996) 293–304.
[39] G.M. Morris, D.S. Goodsell, R.S. Halliday, R. Huey, W.E. Hart, R.K. Belew, A.J. Olson, Automated docking using a Lamarckian genetic algorithm and an empirical binding free energy function, Journal of Computational Chemistry 19 (1998) 1639–1662.
[40] W. Humphrey, A. Dalke, K. Schulten, VMD: visual molecular dynamics, Journal of Molecular Graphics 14 (1996) 33–38.
[41] E. Lindahl, B. Hess, D. van der Spoel, GROMACS 3.0: a package for molecular simulation and trajectory analysis, Journal of Molecular Modeling 7 (2001) 306–317.
[42] B.S. Avvaru, C.U. Kim, K.H. Sippel, S.M. Gruner, M. Agbandje-McKenna, D.N. Silverman, R. McKenna, A short, strong hydrogen bond in the active site of human carbonic anhydrase II, Biochemistry 49 (2010) 249–251.
[43] A.W. Schuttelkopf, D.M. van Aalten, PRODRG: a tool for high-throughput crystallography of protein-ligand complexes, Acta Crystallographica. Section D, Biological Crystallography 60 (2004) 1355–1363.
[44] H.J.C. Berendsen, J.P.M. Postma, W.F. van Gunsteren, A. Di Nola, J.R. Haak, Molecular dynamics with coupling to an external bath, Journal of Chemical Physics 81 (1984) 3684–3690.
[45] M. Parrinello, A. Rahman, Crystal structure and pair potentials: a molecular-dynamics study, Physical Review Letters 45 (1980) 1196–1199.
[46] M. Parrinello, A. Rahman, Polymorphic transitions in single crystals: a new molecular dynamics method, Journal of Applied Physics 52 (1981) 7182–7190.
[47] B. Hess, H. Bekker, H.J.C. Berendsen, J.G.E.M. Fraaije, LINCS: a linear constraint solver for molecular simulations, Journal of Computational Chemistry 18 (1998) 1463–1472.
[48] T. Darden, D. York, L. Pedersen, Particle mesh Ewald: an N Log (N) method for Ewald sums in large systems, Journal of Chemical Physics 98 (1993) 1463–1472.
[49] M. Vinoba, M. Bhagiyalakshmi, S.K. Jeong, S.C. Nam, Y. Yoon, Carbonic anhydrase immobilized on encapsulated magnetic nanoparticles for CO2 sequestration, Chemistry 18 (2012) 12028–12034.
[50] S.M. Gould, D.S. Tawfik, Directed evolution of the promiscuous esterase activity of carbonic anhydrase II, Biochemistry 44 (2005) 5444–5452.
[51] T. Palmer, Understanding Enzyme, 3rd ed. Ellis Horwood, London, 1999.
[52] C.M. Maupin, R. McKenna, D.N. Silverman, G.A. Voth, Elucidation of the proton transport mechanism in human carbonic anhydrase II, Journal of the American Chemical Society 131 (2009) 7598–7608.
[53] D.N. Silverman, R. McKenna, Solvent-mediated proton transfer in catalysis by carbonic anhydrase, Accounts of Chemical Research 40 (2007) 669–675.
[54] S.Y. Venyaminov, J.T. Yang, Circular Dichroism and Conformation Analysis of Biomolecules, Plenum Press, New York, 1996.
[55] L. Stryer, Fluorescence spectroscopy of proteins, Science 162 (1968) 526–533.
[56] C. Temperini, A. Scozzafava, C.T. Supuran, Carbonic anhydrase activation and the drug design, Current Pharmaceutical Design 14 (2008) 708–715.
[57] V.M. Krishnamurthy, G.K. Kaufman, A.R. Urbach, I. Gitlin, K.L. Gudiksen, D.B. Weibel, G.M. Whitesides, Carbonic anhydrase as a model for biophysical and physical-organic studies of proteins and protein-ligand binding, Chemical Reviews 108 (2008) 946–1051.